

# Residual minimization for goal-oriented adaptivity

Sergio Rojas<sup>a,\*</sup>, David Pardo<sup>b,c,d</sup>, Pouria Behnoudfar<sup>a</sup>, Victor M. Calo<sup>a,e</sup>

<sup>a</sup>*School of Earth and Planetary Sciences, Curtin University, Kent Street, Bentley, Perth, WA 6102, Australia*

<sup>b</sup>*University of the Basque Country (UPV/EHU), Leioa, Spain*

<sup>c</sup>*BCAM - Basque Center for Applied Mathematics, Bilbao, Spain*

<sup>d</sup>*IKERBASQUE, Basque Foundation for Science, Bilbao, Spain*

<sup>e</sup>*Mineral Resources, Commonwealth Scientific and Industrial Research Organisation (CSIRO), Kensington, Perth, WA 6152, Australia*

---

## Abstract

In [12], the authors introduce an adaptive, stabilized finite element method (FEM), which solves a stable saddle-point problem. The method delivers a stable continuous approximation and projects the residual onto a broken polynomial space. This projection delivers a reliable error estimate that drives mesh refinement by minimizing a discrete energy norm. In this work, we extend this framework to goal-oriented adaptivity (GoA). We solve the primal and adjoint problems using the same initial saddle-point formulation, but with different right-hand sides. Additionally, we obtain two alternative error estimates, which are efficient to guide refinements. Several numerical examples illustrate the framework's performance on diffusion-advection-reaction problems.

**Keywords:** goal-oriented adaptivity, stabilized finite elements, residual minimization, inf-sup stability, discontinuous Galerkin  
**2010 MSC:** 65N12, 65N30, 76M10

---

## 1. Introduction

Adaptive mesh refinement seeks to minimize the computational effort required to obtain solutions of boundary value problems when using grid-based numerical methods. In this class of methods, it is customary to perform refinements in order to minimize the error in an energy norm of the problem (see e.g., [5]). This energy-norm-driven mesh adaptivity considerably reduces the computational cost of the numerical simulations. Nevertheless, this adaptive strategy is often impractical, since many engineering applications seek only to approximate a particular quantity of interest (QoI).

In the late 90's, goal-oriented adaptivity (GoA) arose to tackle this problem (see, e.g., [7, 40, 39, 44, 30, 15]). In GoA, we first construct an adjoint problem (see [39]).

---

\* Corresponding author

Email address: srojash@gmail.com (Sergio Rojas)

Then, we represent the error in the quantity of interest as an integral over the entire computational domain that depends upon the solution of both direct and adjoint problems. Finally, we use the direct and adjoint solutions to build adequate a posteriori error estimators.

The main limitation of classical finite element methods is that they can suffer from instability on coarse meshes. Thus, adaptivity with standard finite elements is not feasible in several scenarios since stability is key for a posteriori error estimation. Several alternative Galerkin methods exist that are stable on coarse meshes (see, e.g., [26, 28, 32] and references therein).

In [12], the authors present an adaptive stabilized finite element method. This method combines the idea of residual minimization, which is at the core of several stabilization methods proposed since the '60s (e.g., Least-Squares Finite Element Method (LS-FEM) [25, 37, 9, 33] and Galerkin/Least-Squares (GaLS) method [31]), and discontinuous Galerkin (dG) methods, where stability is achieved by enlarging the continuous trial space with discontinuous functions, and adding penalization terms (see [41, 36, 34, 14, 10, 27], and [21] for a recent overview).

The formulation of [12] minimizes a discrete residual in a dG norm. It starts from an inf-sup stable dG formulation and minimizes the residual in an adjoint norm (to the dG test functions) over a trial space of conforming functions (i.e., a standard finite element space). Solving the residual minimization problem is equivalent to solving a saddle-point problem that inherits the dG inf-sup stability. As a consequence, the method delivers solutions of the same quality as those associated with the underlying dG formulation. From the practical point of view, the resulting mixed formulation delivers two significant benefits: A stable approximation of the solution in the trial space of continuous (conforming) functions, and a projection of the residual onto the discontinuous dG test space (error estimate). This method has similarities with the Discontinuous Petrov–Galerkin (DPG) methods since both technologies minimize the residual in a non-standard norm (see, e.g., [16, 19, 17, 45, 20, 13], and [18] for a general overview). The main difference between the methodologies is that the starting point is a non-conforming formulation. The non-conformity of the discretization allows us to use stronger norms when the trial space contains continuous functions.

In this work, we extend the method proposed in [12] to goal-oriented adaptivity (GoA). We propose and analyse a general theory that applies to any problem where a well-posed discontinuous Galerkin formulation for the primal problem is available. We set the corresponding discrete adjoint problem as an adequate saddle-point problem, where the solution for the adjoint problem belongs to the discontinuous test space. The same dG inf-sup arguments guarantee the well-posedness of the adjoint saddle-point problem. Solving both the primal and the adjoint problem requires the solution of a single saddle-point problem with two right-hand sides. Unfortunately, the extra variable in the adjoint formulation that belongs to the continuous trial space does not estimate the residual. To overcome this problem, we propose two alternatives that solve additional reduced problems. This GoA strategy is similar to a recent DPG theory [35], where they solve the adjoint problem in terms of the initial saddle-point with a different right-hand side. The idea of considering a conforming approximation of the primal problem, together with a dG

approximation of the adjoint problem, has also been considered in [38], where the GoA estimators are obtained by combining the dual-weighted residual method and equilibrated-flux reconstruction methods.

The rest of the paper goes as follows, in Section 2 we introduce the associated direct problems; the continuous problem with its dG formulation (Section 2.1), and the direct saddle-point formulation coming from the AS-FEM (Section 2.2). In Section 3 we present the adjoint problems; the adjoint continuous problems with its adjoint dG formulation (Section 3.1), the adjoint saddle-point formulation (Section 3.2), and the residual representative for the adjoint saddle-point formulation (Section 5). In Section 4, we introduce the main idea behind the proposed GoA strategy. In Section 5 we give the mathematical fundamentals of steps 3-4 of the methodology presented in Section 4. In Section 6, we introduce the diffusion-advection-reaction model problem, including its continuous weak formulation and a discontinuous Galerkin formulation, with the spirit of facilitating the understanding of the framework introduced in the previous sections. In Section 7, we show the performance of the method through adequate numerical examples in the diffusion-advection-reaction context. Section 8 details our conclusions and further lines of work.

## 2. Direct problems

In this section, we introduce the problems (in abstract sense) that define the theory behind our methodology. Section 2.1 describes the continuous problem and a consistent discontinuous Galerkin formulation to approximate it. Section 2.2 briefly describes the residual minimization analyzed in [12].

### 2.1. Continuous and dG formulations

Let  $U, V$  be real Banach spaces, and  $V$  be reflexive. We want to obtain an accurate approximation of a quantity of interest  $q(u)$ , where  $q : U \rightarrow \mathbb{R}$  is a bounded linear operator. The function  $u \in U$  is the analytical solution of a well-posed weak formulation of the form (continuous direct problem):

$$\begin{cases} \text{Find } u \in U, \text{ such that:} \\ b(u, v) = l(v), \quad \forall v \in V, \end{cases} \quad (1)$$

with  $b : U \times V \rightarrow \mathbb{R}$ , and  $l : U \rightarrow \mathbb{R}$  being a bounded bilinear, and bounded linear operator, respectively.

We consider a discrete space  $V_h$ , not necessarily conforming with either  $U$  or  $V$  (typically a broken polynomial space). Assume that the continuous problem (1) admits a discrete variational formulation of the form:

$$\begin{cases} \text{Find } u_h^{\text{dG}} \in V_h, \text{ such that:} \\ b_h(u_h^{\text{dG}}, v_h) = l_h(v_h), \quad \forall v_h \in V_h, \end{cases} \quad (2)$$

being inf-sup stable with respect to a given norm  $\|\cdot\|_{V_h}^2 := (\cdot, \cdot)_{V_h}$  [27, 21]. Thus, it satisfies the following Assumption:

**Assumption 1** (Inf-sup stability). *The space  $V_h$  can be equipped with a norm  $\|\cdot\|_{V_h}$ , and there exists a mesh independent constant  $C_{sta} > 0$ , such that:*

$$\sup_{0 \neq v_h \in V_h} \frac{b_h(w_h, v_h)}{\|v_h\|_{V_h}} \geq C_{sta} \|w_h\|_{V_h}, \quad \forall w_h \in V_h. \quad (3)$$

We also assume the following:

**Assumption 2** (Strong consistency with regularity). *The exact solution  $u$  of problem (1) belongs to a subspace  $U_\# \subset U$  such that the discrete bilinear form  $b_h$  supports evaluations in the extended space  $V_{h,\#} \times V_h$ , with  $V_{h,\#} := U_\# + V_h$ , and the following holds true:*

$$b_h(u, v_h) = l_h(v_h), \quad \forall v_h \in V_h. \quad (4)$$

**Assumption 3** (Boundedness). *The stability norm  $\|\cdot\|_{V_h}$  can extend to the space  $V_{h,\#}$  defined in Assumption 2. Moreover, there is a second norm  $\|\cdot\|_{V_{h,\#}}$  on  $V_{h,\#}$  satisfying the following two properties:*

- (i)  $\|v\|_{V_h} \leq \|v\|_{V_{h,\#}}$ , for all  $v \in V_{h,\#}$ ,
- (ii) *there exists a mesh independent constant  $C_{bnd} < \infty$ , such that:*

$$b_h(w, v_h) \leq C_{bnd} \|w\|_{V_{h,\#}} \|v_h\|_{V_h}, \quad \forall (w, v) \in V_{h,\#} \times V_h. \quad (5)$$

Assumptions 1-3 are the standard for consistent dG formulations. Assumption 1 is sufficient to guarantee well-posedness for the discrete problem (2), while assumptions 2 and 3 guarantee the following a priori error estimate (see [21]):

$$\left\| u - u_h^{\text{dG}} \right\|_{V_h} \leq \left( 1 + \frac{C_{bnd}}{C_{sta}} \right) \inf_{v_h \in V_h} \|u - v_h\|_{V_{h,\#}}. \quad (6)$$

## 2.2. Mixed direct problem

Rather than solving the discrete problem (2), the residual minimization on a dual dG norm [12] approximates the dG solution  $u_h^{\text{dG}} \in V_h$  in a proper subspace  $U_h \subset V_h$ . In particular, we select a conforming subspace in  $U$ . Thus, the discrete problem becomes: solve the following residual minimization problem,

$$\begin{cases} \text{Find } u_h \in U_h \subset V_h, \text{ such that:} \\ u_h = \arg \min_{w_h \in U_h} \frac{1}{2} \|l_h(\cdot) - b_h(w_h, \cdot)\|_{V_h^*}^2 = \arg \min_{w_h \in U_h} \frac{1}{2} \|R_{V_h}^{-1} B_h(u_h^{\text{dG}} - w_h)\|_{V_h}^2. \end{cases} \quad (7)$$

In the above, the operator  $B_h$  is:

$$B_h : \begin{cases} V_h \rightarrow V_h^* \\ w_h \rightarrow b_h(w_h, \cdot), \end{cases} \quad (8)$$

$R_{V_h}^{-1}$  denotes the inverse of the Riesz map:

$$\begin{aligned} R_{V_h} & : V_h \rightarrow V_h^* \\ \langle R_{V_h} y_h, v_h \rangle_{V_h^* \times V_h} & := (y_h, v_h)_{V_h}, \end{aligned} \quad (9)$$

and the dual norm  $\|\cdot\|_{V_h^*}$  is:

$$\|\phi\|_{V_h^*} := \sup_{0 \neq w \in W} \frac{\langle \phi, w \rangle_{V_h^* \times V_h}}{\|w\|_{V_h}}, \quad \forall \phi \in V_h^*. \quad (10)$$

The second equality in (7) holds since the Riesz operator is isometric and isomorphism and satisfies:

$$\|\phi\|_{V_h^*} = \|R_{V_h}^{-1} \phi\|_{V_h}, \quad \forall \phi \in V_h^*, \quad (11)$$

and the dG solution of the discrete problem (2) satisfies  $l_h(\cdot) = B_h u_h^{\text{dG}}$  in  $V_h^*$ .

Problem (7) is equivalent to the following saddle-point problem (cf., [12]):

$$\begin{cases} \text{Find } (\varepsilon_h, u_h) \in V_h \times U_h, \text{ such that:} \\ (\varepsilon_h, v_h)_{V_h} + b_h(u_h, v_h) = l_h(v_h), & \forall v_h \in V_h, \\ b_h(w_h, \varepsilon_h) = 0, & \forall w_h \in U_h, \end{cases} \quad (12)$$

where  $\varepsilon_h \in V_h$  denotes a residual representative in terms of  $u_h^{\text{dG}} \in V_h$  and  $u_h \in U_h \subset V_h$ . Indeed, using the Riesz representation, the first condition in Equation (12) is equivalent to:

$$\varepsilon_h = R_{V_h}^{-1} (l_h(\cdot) - b_h(u_h, \cdot)) = R_{V_h}^{-1} B_h (u_h^{\text{dG}} - u_h). \quad (13)$$

Solving the saddle-point problem (12) has several benefits. First, looking for a solution in a subspace of the discontinuous space  $V_h$  allows us to extract explicitly certain properties of the discrete solution. For example, we can obtain continuous solutions without postprocessing the dG solution. Also, the saddle-point problem inherits the discrete stability of the dG formulation. Moreover, the error estimate is efficient and reliable. Below, we formalize these claims (see [12]):

**Theorem 1** (A priori bounds and error estimates). *When assumptions 1-3 are satisfied, the mixed problem (12) has a unique solution  $(\varepsilon_h, u_h) \in V_h \times U_h$ . Moreover, such solution satisfies the following a priori bounds:*

$$\|\varepsilon_h\| \leq \|l_h\|_{V_h^*} \quad \text{and} \quad \|u_h\|_{V_h} \leq \frac{1}{C_{sta}} \|l_h\|_{V_h^*}, \quad (14)$$

and the following a priori error estimate holds true:

$$\|u - u_h\|_{V_h} \leq \left(1 + \frac{C_{bnd}}{C_{sta}}\right) \inf_{w_h \in U_h} \|u - w_h\|_{V_{h,\#}}, \quad (15)$$

recalling that  $u \in V_{\#}$  is the exact solution to the continuous direct problem (1).

**Proposition 1** (Efficiency of the residual representative). *Under the same hypotheses of Theorem 1, it follows:*

$$\|\varepsilon_h\|_{V_h} \leq C_{bnd} \|u - u_h\|_{V_{h,\#}}. \quad (16)$$

Assume that one of the following additional assumptions is satisfied:

**Assumption 4** (Saturation). *Let  $u_h \in U_h$  be the second component of the pair  $(\varepsilon_h, u_h) \in V_h \times U_h$  solving (12) and let  $u_h^{dG} \in V_h$  be the unique solution to (2). There exists a real number  $\delta_s \in [0, 1)$ , uniform with respect to the mesh size, such that*

$$\|u - u_h^{dG}\|_{V_h} \leq \delta_s \|u - u_h\|_{V_h}.$$

**Assumption 5** (Weak saturation). *Let  $u_h \in U_h$  be the second component of the pair  $(\varepsilon_h, u_h) \in V_h \times U_h$  solving (12) and let  $u_h^{dG} \in V_h$  be the unique solution to (2). There exists a real number  $\delta_w > 0$ , uniform with respect to the mesh size, such that*

$$\|u - u_h^{dG}\|_{V_h} \leq \delta_w \|u_h^{dG} - u_h\|_{V_h}.$$

Then, the following result holds true:

**Proposition 2** (Reliability of the residual representative). *Under the same hypotheses of Theorem 1, it holds:*

$$\|u_h^{dG} - u_h\|_{V_h} \leq \frac{1}{C_{\text{sta}}} \|\varepsilon_h\|_{V_h}. \quad (17)$$

Moreover, when the solution satisfies either of the saturation Assumptions 4 or 5, then the following a posteriori error estimate holds:

$$\|u - u_h\|_{V_h} \leq \frac{C_{\text{sat}}}{C_{\text{sta}}} \|\varepsilon_h\|_{V_h}, \quad (18)$$

with  $C_{\text{sat}} = \frac{1}{1 - \delta_s}$  if Assumption 4 is satisfied, and  $C_{\text{sat}} = \delta_w$  if only the weaker Assumption 5 is satisfied.

**Remark 1** (On the discrete assumptions). *The Assumption 4 is not standard in the dG theory as it involves the discrete solution  $u_h \in U_h$ . This assumption states that the discrete approximation  $u_h^{dG}$  is uniformly closer than  $u_h$  to the analytical solution  $u$  with respect to the norm in  $V_h$ . Assumption 4 is satisfied when the dG a priori estimate (6) is optimal (i.e., when the norms  $\|\cdot\|_{V_h}$  and  $\|\cdot\|_{V_{h,\#}}$  are equivalent) due to the a priori error estimate for  $u_h$  (15), and the fact that  $U_h$  is a subspace of  $V_h$ . This assumption is expected to be asymptotically satisfied when the estimate (6) is quasi-optimal (i.e., when the norms are not equivalent but the left and right quantities in (6) decay with the same rate). The Assumption 5 is a weaker version of Assumption 4, since the later implies Assumption 5, while the reciprocal only is granted when  $\delta_w < 1/2$ .*

### 3. Adjoint problems

In this section, we introduce the adjoint (dual) problems. Section 3.1 discusses the adjoint continuous formulation and its dG formulation. Section 3.2 introduces the adjoint problem to the saddle-point formulation (12).

### 3.1. Continuous and dG adjoint formulations

We want to accurately approximate a quantity of interest  $q(u)$ , where  $q : U \rightarrow \mathbb{R}$  is a bounded linear operator, and  $u \in U$  is the analytical solution of the continuous, direct problem (5).

The GoA strategy considers a second continuous problem, known as the continuous adjoint problem:

$$\begin{cases} \text{Find } v^* \in V, \text{ such that:} \\ b(w, v^*) = q(w), \quad \forall w \in U, \end{cases} \quad (19)$$

Let operator  $q$  satisfy the following assumption:

**Assumption 6** (Goal extension). *The linear and bounded operator  $q : U \rightarrow \mathbb{R}$  can be extended, and exactly represented in the adjoint space  $V_h^*$ .*

Then, the dG adjoint formulation associated with (1) reads:

$$\begin{cases} \text{Find } v_h^{\text{dG},*} \in V_h, \text{ such that:} \\ b_h(v_h, v_h^{\text{dG},*}) = q(v_h), \quad \forall v_h \in V_h, \end{cases} \quad (20)$$

where  $b(\cdot, \cdot)$  and  $b_h(\cdot, \cdot)$  denote the same bilinear forms coming from the continuous (1) and discrete (2) direct problems, respectively.

We also consider the following assumption:

**Assumption 7** (Strong adjoint consistency with regularity). *The exact solution  $v^*$  of problem (19) belongs to a subspace  $V_\# \subset V$  such that the discrete bilinear form  $b_h$  supports evaluations in the extended space  $V_{h,\#} \times V_{h,\#\#}$ , where  $V_{h,\#}$  is the space defined in Assumption 2 and  $V_{h,\#\#} := V_\# + V_h$ . Moreover, the following identity holds:*

$$b_h(w, v^*) = q(w), \quad \forall w \in V_{h,\#}. \quad (21)$$

Assumption 7 implies the following identity:

$$q(u - u_h^{\text{dG}}) = b_h(u - u_h^{\text{dG}}, v^*) = b_h(u - u_h^{\text{dG}}, v^* - v_h^{\text{dG},*}), \quad (22)$$

where the last equality follows from the Galerkin orthogonality.

Standard GoA algorithms employ a posteriori error estimates of the quantity of interest (22). These estimates provide an upper bound for (22) in terms of locally computable variables that guide the adaptivity and controls the error in the quantity  $q(u - u_h^{\text{dG}})$ . The main limitation with the a posteriori procedure is that the adjoint consistency Assumption 7 is not always satisfied for all consistent dG formulations (cf. [3]). This limitation implies that the number of suitable dG formulations for GoA is limited.

**Remark 2** (Well-posedness of the dG problem). *Assumption 6 guarantees the well-posedness for the dG adjoint problem (20) since the discrete inf-sup condition (3) is equivalent to (see [8]):*

$$\sup_{0 \neq w_h \in V_h} \frac{b_h(w_h, v_h)}{\|w_h\|_{V_h}} \geq C_{\text{sta}} \|v_h\|_{V_h}, \quad \forall v_h \in V_h. \quad (23)$$

### 3.2. Mixed adjoint formulation

Consider the following adjoint saddle-point problem:

$$\begin{cases} \text{Find } (v_h^*, w_h^*) \in V_h \times U_h, \text{ such that :} \\ (v_h^*, v_h)_{V_h} + b_h(w_h^*, v_h) = 0, & \forall v_h \in V_h, \\ b_h(w_h, v_h^*) = q(w_h), & \forall w_h \in U_h, \end{cases} \quad (24)$$

The discrete solution  $u_h$  of problem (12) belongs to  $U_h \subset V_h$ , therefore its adjoint pair  $v_h^* \in V_h$  satisfies:

$$b_h(w_h, v_h^*) = q(w_h), \quad \forall w_h \in U_h, \quad (25)$$

which is the second equation in (24). The saddle-point formulation for the direct problem (12) is equivalent to a residual minimization. Similarly, the adjoint formulation minimizes the Riesz representation subject to constraints. If the direct saddle-point problem (12) is well-posed, then the mixed-adjoint problem (24) is also well-posed, as both discrete problems share the same left-hand side square matrix.

**Remark 3** (Constrained Riesz representer minimization). *We seek the optimal Riesz representer  $v_h^* \in V_h$  subject to the constraint (25). To analyze this problems as an unconstrained optimization problem, we introduce a Lagrangian and the respective set of multipliers  $w_h \in U_h$ . Let  $(v_h^*, w_h^*) \in V_h \times U_h$  be a stationary point of*

$$\mathcal{L}(v_h, w_h) = \frac{1}{2}(v_h, v_h)_{V_h} + b_h(w_h, v_h) - q(w_h).$$

*The stationarity conditions of  $\mathcal{L}(v_h, w_h)$  (i.e.,  $\frac{\partial \mathcal{L}(v_h, w_h)}{\partial v_h} = 0$  and  $\frac{\partial \mathcal{L}(v_h, w_h)}{\partial w_h} = 0$ ) correspond to the mixed adjoint problem (24). Denoting the stationary value of the Lagrangian  $\mathcal{L}^*(q) = \mathcal{L}(v_h^*, w_h^*) = \frac{1}{2}(v_h^*, v_h^*)_{V_h}$  as an implicit function of quantity of interest, then  $-w_h^*$  determines the (marginal) effect of the each constraint on the attainable value of the Riesz representer.*

**Remark 4** (Petrov-Galerkin method with optimal trial functions). *The first equation in (24) introduces a Lagrange multiplier  $w_h^* \in U_h$  (see Remark 3). This allows us to equivalently express (24) in terms of the adjoint discrete solution  $v_h^* \in V_h$  via the following Petrov-Galerkin problem:*

$$\begin{cases} \text{Find } v_h^* \in \Theta_h, \text{ such that:} \\ b_h(w_h, v_h^*) = q(w_h), \quad \forall w_h \in U_h, \end{cases} \quad (26)$$

where the discrete space  $\Theta_h \in V_h$  is defined as:

$$\Theta_h := \{\varphi_h \in V_h \text{ s.t. } \exists w_h \in U_h : (\varphi_h, v_h)_{V_h} + b_h(w_h, v_h) = 0, \forall v_h \in V_h\}. \quad (27)$$

*This subspace is the Riesz representation of the action of  $b_h$  on each basis of  $U_h$ . Problem (24) inherits the well-posedness from the direct saddle-point problem (12). The well-posedness of problem (26) is a direct consequence of the inf-sup Assumption 1. Moreover, the existence of a unique representative  $w_h \in U_h$  in the definition (27) is a consequence of the bijectivity of the Riesz isomorphism and the injectivity of the operator  $B_h$  (see Equation (8)), implying that  $w_h^* \in U_h$  is the unique representative of  $v_h^*$  in  $\Theta_h$ .*



### 3.3. Residual based error representative for the adjoint problem

Unlike the saddle-point formulation of the direct problem (12), the adjoint saddle-point formulation does not deliver an on-the-fly error estimate, as  $w_h^* \in U_h$  is a Lagrange multiplier. Nevertheless, we can estimate the error by solving the following discrete problem:

$$\begin{cases} \text{Find } \varepsilon_h^* \in V_h, \text{ such that:} \\ (\varepsilon_h^*, v_h)_{V_h} = q(v_h) - b_h(v_h, v_h^*), \quad \forall v_h \in V_h. \end{cases} \quad (28)$$

which estimates the distance from the residual in  $V_h$  to its orthogonal projection onto the optimal trial function space. This problem has a unique solution and is well posed as we discuss below.

**Remark 5.** If  $U_h$  is strictly contained in  $V_h$  then, in general,  $\varepsilon_h^* \neq 0$  in  $V_h^*$ . Indeed, the orthogonality constraint  $(\varepsilon_h^*, v_h)_{V_h} = 0$  holds only if  $v_h \in U_h$ . Therefore, equation (28), together with identity (25), imply that  $\varepsilon_h^* = R_{V_h}^{-1} B_h^*(v_h^{dG,*} - v_h^*)$ , with  $B_h^*$  defined as:

$$\begin{aligned} B_h^* : \quad V_h &\rightarrow V_h^* \\ v_h &\rightarrow b_h(\cdot, v_h). \end{aligned} \quad (29)$$

Unlike the residual representative for the direct problem  $\varepsilon_h$  (see (13)), the adjoint error representative  $\varepsilon_h^*$  (see (29)) may be inefficient as error estimator. Nevertheless, the following reliability result holds:

**Theorem 2** (Reliability of the adjoint residual representative). *Let  $v_h^* \in V_h$  be the first component of the solution pair  $(v_h^*, w_h^*) \in V_h \times U_h$  of (24). Let  $v_h^{dG,*} \in V_h$  be the unique solution to (20). Then:*

$$\|v_h^{dG,*} - v_h^*\|_{V_h} \leq \frac{1}{C_{sta}} \|\varepsilon_h^*\|_{V_h}. \quad (30)$$

*Proof.* We have

$$\begin{aligned} \|\varepsilon_h^*\|_{V_h} &= \|R_{V_h}^{-1} B_h^*(v_h^{dG,*} - v_h^*)\|_{V_h^*} && \text{(by (28) and (20))} \\ &= \sup_{0 \neq v_h \in V_h} \frac{b_h(v_h, v_h^{dG,*} - v_h^*)}{\|v_h\|_{V_h}} \\ &\geq C_{sta} \|v_h^{dG,*} - v_h^*\|_{V_h}, && \text{(by (23))} \end{aligned}$$

proving (30).  $\square$

## 4. Goal-oriented-adaptivity algorithm

In the proposed methodology, rather than solving problems (2) and (20), we consider an adequate subspace  $U_h \subset V_h$  for the discrete approximation, for instance a conforming subspace with the same capacity properties for the solution as  $V_h$  (cf., [12, Remark 5]), and perform the following four steps:

1. **Direct problem:** We solve the mixed direct Galerkin formulation (see Section 2.2):

$$\begin{cases} \text{Find } (\varepsilon_h, u_h) \in V_h \times U_h, \text{ such that :} \\ (\varepsilon_h, v_h)_{V_h} + b_h(u_h, v_h) = l_h(v_h), & \forall v_h \in V_h, \\ b_h(w_h, \varepsilon_h) = 0, & \forall w_h \in U_h, \end{cases}$$

where  $u_h$  approximates the discrete direct problem (2), and  $\varepsilon_h$  represents a projection in  $V_h$  of the discrete residual (as functional in the adjoint space  $V_h^*$ ).

2. **Adjoint problem:** We solve the following mixed adjoint Galerkin formulation (see Section 3.2):

$$\begin{cases} \text{Find } (v_h^*, w_h^*) \in V_h \times U_h, \text{ such that :} \\ (v_h^*, v_h)_{V_h} + b_h(w_h^*, v_h) = 0, & \forall v_h \in V_h, \\ b_h(w_h, v_h^*) = q(w_h), & \forall w_h \in U_h, \end{cases}$$

where  $v_h^*$  is an approximation of the discrete solution  $v_h^{\text{dG},*}$  of problem (20) satisfying  $b_h(\cdot, v_h^*) = q(\cdot)$  in  $U_h^* \supset V_h^*$ , while  $w_h^*$  is a Lagrange multiplier.

3. **Residual estimation:** We estimate a localizable upper bound for  $q(u - u_h)$  using one of the following two estimators (see Section 5):

- a) **Adjoint residual based estimator.** We first compute the solution of the following discrete problem:

$$\begin{cases} \text{Find } \varepsilon_h^* \in V_h, \text{ such that :} \\ (\varepsilon_h^*, v_h)_{V_h} = q(v_h) - b_h(v_h, v_h^*), & \forall v_h \in V_h, \end{cases}$$

representing a projection of the discrete adjoint residual in  $V_h$  through the Riesz operator (9). Then, we estimate an upper bound of the quantity  $q(u - u_h)$  in terms of the value  $(\varepsilon_h, \varepsilon_h^*)_{V_h}$ .

- b) **Adjoint dG based estimator.** We first solve problem (20) to obtain explicitly  $v_h^{\text{dG},*}$ . Then, we estimate an upper bound of the quantity  $q(u - u_h)$  in terms of the value  $(\varepsilon_h, v_h^{\text{dG},*} - v_h^*)_{V_h}$ .

4. **Local estimation:** We first estimate over each element a local contribution of the error indicator of Step 3 by using a localizable representation  $E(\cdot, \cdot)$  of the inner product  $(\cdot, \cdot)_{V_h}$ , satisfying (see Section 5.1):

$$|(v_h, z_h)_{V_h}| \leq E(v_h, z_h), \quad \forall v_h, z_h \in V_h. \quad (31)$$

Then, we use this local estimate to guide the goal oriented adaptivity by using the Dörfler bulk-chasing marking criterion (see [24]). The strategy first orders in a decreasing order the local error estimates. Then, it marks for refinement the elements for which the cumulative sum remains smaller than a given percentage of the total error estimate.

This procedure requires no further a posteriori error estimation. Additionally, steps 1 and 2 require the solution of the same saddle-point system. Thus, the problem becomes a single system with multiple right-hand sides. Finally, this process does

not require the standard adjoint consistency Assumption 7, since we obtain upper bounds in terms of the dG discrete solutions. This subtle insight significantly enlarges the range of available formulations that we can apply to this class of problems.

## 5. Goal oriented a posteriori error estimation

In this section, we present the a posteriori error estimation that we employ to define the localizable error estimations to guide the GoA. We obtain estimations in terms of the dG solutions associated with problems (2) and (20). Therefore, they are based in the discrete stability of the involved problems.

We first prove two propositions, which encapsule useful relations in terms of the involved discrete terms.

**Proposition 3** (Discrete orthogonality). *Let  $u_h^{dG}$ ,  $(\varepsilon_h, u_h)$ ,  $v_h^{dG,*}$  and  $(v_h^*, w_h)$  be the unique solution of problems (2), (12), (20), and (24), respectively. Then, the following equalities hold:*

- a)  $b_h(u_h, v_h^{dG,*} - v_h^*) = 0$
- b)  $(v_h^*, \varepsilon_h)_{V_h} = 0$
- c)  $q(u_h) - l_h(v_h^*) = 0$
- d)  $b_h(u_h^{dG} - u_h, v_h^*) = 0$

*Proof.* Equality a) is a direct consequence of the identities (20) and (25). Since  $v_h^* \in V_h$ , using the first equation in (24), and the second equation in (12), respectively, we obtain:

$$(v_h^*, \varepsilon_h)_{V_h} = -b_h(w_h, \varepsilon_h) = 0,$$

proving b). To prove c), we consider the second equation in (24), the first equation in (12) and the result in b). Finally, d) is a consequence of the first equation in (12), the identity (2), and the symmetry of the discrete inner product in  $V_h$ .  $\square$

**Proposition 4** (Error in the goal). *Under the same hypotheses of Proposition 3, the following identity holds:*

$$q(u_h^{dG} - u_h) = b_h(u_h^{dG} - u_h, v_h^{dG,*} - v_h^*) = l_h(v_h^{dG,*} - v_h^*). \quad (32)$$

*If in addition the adjoint Assumption 7 is satisfied, then it holds:*

$$q(u - u_h) = b_h(u - u_h, v^* - v_h^*) = l_h(v^* - v_h^*). \quad (33)$$

*Proof.* Using (20) and the bilinearity of the operator  $b_h$ , we obtain:

$$q(u_h^{dG} - u_h) = b_h(u_h^{dG} - u_h, v_h^{dG,*} - v_h^*) + b_h(u_h^{dG} - u_h, v_h^*).$$

The first equality in (32) is a consequence of d) in Proposition 3. Following a similar strategy, to obtain the second equality we employ the identity a) of Proposition 3. Finally, (33) is a direct consequence of the adjoint consistency Assumption 7, and the identity  $b_h(u_h, v^* - v_h^*) = b_h(u_h, v_h^{dG,*} - v_h^*) = 0$ .  $\square$

In the following, we explore a posteriori error bounds in terms of the discrete solutions. An immediate consequence of the reliability of the residual representative  $\varepsilon_h$  (see Proposition 2) is:

**Proposition 5** (First a posteriori GoA error estimator). *Let  $u_h^{dG}$  and  $(\varepsilon_h, u_h)$  be the unique solution of problems (2) and (12), respectively. It holds:*

$$\left| q(u_h^{dG} - u_h) \right| \leq \frac{1}{C_{sta}} \|q\|_{V_h^*} \|\varepsilon_h\|_{V_h}. \quad (34)$$

Moreover, if the saturation Assumption 4 is satisfied, then:

$$\left| q(u - u_h) \right| \leq \frac{1}{C_{sta}(1 - \delta_s)} \|q\|_{V_{h,\#}^*} \|\varepsilon_h\|_{V_h}, \quad (35)$$

while if Assumption 4 is not satisfied, but the weaker condition of Assumption 5 is satisfied, it holds:

$$\left| q(u - u_h) \right| \leq \frac{1 + \delta_w}{C_{sta}} \|q\|_{V_{h,\#}^*} \|\varepsilon_h\|_{V_h}, \quad (36)$$

where  $u$  denotes the analytical solution of problem (1),  $V_{h,\#}$  is the space defined in Assumption 2 and  $\|\cdot\|_{V_{h,\#}^*}$  denotes the extension of the adjoint norm  $\|\cdot\|_{V_h^*}$ , defined in (10), to the adjoint space of  $V_{h,\#}$ .

Even if inequality (34) implies that the error in the estimation of  $q(u_h^{dG} - u_h)$  is controlled by  $\varepsilon_h$ , this estimation ignores the contribution of the adjoint saddle-point problem. Motivated by Assumptions 4 and 5, we consider the following additional assumptions:

**Assumption 8** (adjoint saturation condition). *Let  $u_h^{dG}$  and  $(\varepsilon_h, u_h)$  be the unique solution of problems (2) and (12), respectively. There exists a mesh independent constant  $\mu_s \in [0, 1)$ , such that  $|q(u - u_h^{dG})| \leq \mu_s |q(u - u_h)|$ .*

**Assumption 9** (adjoint weak condition). *Let  $u_h^{dG}$  and  $(\varepsilon_h, u_h)$  be the unique solution of problems (2) and (12), respectively. There exists a mesh independent constant  $\mu_w > 0$ , such that  $|q(u - u_h^{dG})| \leq \mu_w |q(u_h^{dG} - u_h)|$ .*

The following result follows:

**Proposition 6** (Second a posteriori GoA error estimator). *Let  $u_h^{dG}$ ,  $(\varepsilon_h, u_h)$ ,  $v_h^{dG,*}$ ,  $(v_h^*, w_h^*)$  be the unique solutions of problems (2), (12), (20), and (24) respectively, and let  $\varepsilon_h^*$  be the a posteriori residual estimator of (28). The following holds true:*

$$\left| q(u_h^{dG} - u_h) \right| = \left| (\varepsilon_h, v_h^{dG,*} - v_h^*)_{V_h} \right| \leq \frac{1}{C_{sta}} \|\varepsilon_h\|_{V_h} \|\varepsilon_h^*\|_{V_h}. \quad (37)$$

Moreover, if the saturation Assumption 8 is satisfied, it holds:

$$\left| q(u - u_h) \right| \leq \frac{1}{1 - \mu_s} \left| (\varepsilon_h, v_h^{dG,*} - v_h^*)_{V_h} \right| \leq \frac{1}{C_{sta}(1 - \mu_s)} \|\varepsilon_h\|_{V_h} \|\varepsilon_h^*\|_{V_h}. \quad (38)$$

while if only the weaker Assumption 9 is satisfied, then:

$$|q(u - u_h)| \leq (1 + \mu_w) \left| (\varepsilon_h, v_h^{dG,*} - v_h^*)_{V_h} \right| \leq \frac{1 + \mu_w}{C_{sta}} \|\varepsilon_h\|_{V_h} \|\varepsilon_h^*\|_{V_h}, \quad (39)$$

with  $u$  being the analytical solution of problem (1).

*Proof.* (37) is a direct consequence of the identity (32), and the bound for the adjoint problem (30). Finally, Equations (38) and (39) are consequence of the triangular inequality  $|q(u - u_h)| \leq |q(u - u_h^{dG})| + |q(u_h^{dG} - u_h)|$ .  $\square$

Proposition 6 is independent of the adjoint consistency Assumption 7 in which the standard dG based a posteriori error analysis for GoA hinges. Moreover, if the adjoint saturation Assumption 8 is satisfied, the following result also holds:

**Corollary 1.** *Under the same hypotheses of Proposition 6, if the adjoint saturation Assumption 8 is satisfied, then:*

$$\left| (\varepsilon_h, v_h^{dG,*} - v_h^*)_{V_h} \right| \leq \frac{1}{1 + \mu_s} |q(u - u_h)|. \quad (40)$$

*Proof.* Direct consequence of the triangular inequality  $|q(u_h^{dG} - u_h)| \leq |q(u - u_h^{dG})| + |q(u - u_h)|$ , and the identity (37).  $\square$

From Proposition 6, we may localize the GoA estimate in terms of the quantity  $|(\varepsilon_h, v_h^{dG,*} - v_h^*)_{V_h}|$ , which requires the solution of (20) to obtain explicitly  $v_h^{dG,*}$ . In turn, solving (20) requires to form and invert an equation system that is different from the saddle-point formulation (12) if the space  $U_h$  is a proper subspace of  $V_h$ . Alternatively, to obtain an upper bound of the quantity  $|(\varepsilon_h, \varepsilon_h^*)_{V_h}|$ , we estimate the error from the following result:

$$\left| |q(u_h^{dG} - u_h)| - |(\varepsilon_h, \varepsilon_h^*)_{V_h}| \right| \leq \left( 1 + \frac{1}{C_{sta}} \right) \|\varepsilon_h\|_{V_h} \|\varepsilon_h^*\|_{V_h}. \quad (41)$$

Obtaining  $\varepsilon_h^*$  also requires to solve one additional problem (see (28)). However, the main advantage is that it requires to invert the precomputed Gram matrix coming from the inner product  $(\cdot, \cdot)_{V_h}$  which is always symmetric and positive definite. Moreover, when using an iterative solver for the saddle-point problem, a preconditioner for the Gram matrix is already available (cf. [12]), which makes the computational cost for obtaining  $\varepsilon_h^*$  significantly lower than that to compute  $\varepsilon_h$ . Effectively, computing  $\varepsilon_h^*$  is equivalent to computing an extra outer loop of the iteration to compute the adjoint problem.

### 5.1. Localizable upper-bound estimates

Since most dG norms are global, we seek to define an adequate local representation to estimate the error to perform goal-oriented adaptivity. Denoting by  $\mathcal{P}_h$  a conforming partition of the domain  $\Omega$  (cf. Section 6.2), we assume that the following assumption is satisfied:

**Assumption 10** (Inner product localization). *For any  $T \in \mathcal{P}_h$ , the inner product  $(\cdot, \cdot)_{V_h}$  admits a local representation  $(\cdot, \cdot)_T$ , such that:*

1.  $(\cdot, \cdot)_T$  is an inner product for  $V_h|_T$ .
2.  $(w_h, v_h)_{V_h} = \sum_{T \in \mathcal{P}_h} (w_h, v_h)_T, \forall w_h, v_h \in V_h$ .

Under Assumption 10, we define the following upper bound for the inner product  $(\cdot, \cdot)_{V_h}$ :

$$E(v_h, w_h) := \sum_{T \in \mathcal{P}_h} \|v_h\|_T \|w_h\|_T, \quad \forall w_h, v_h \in V_h, \quad (42)$$

with  $\|\cdot\|_T^2 := (\cdot, \cdot)_T$ . The following result is a direct consequence of the triangular and Cauchy-Schwarz inequalities and of Proposition 6.

**Proposition 7** (Upper bound of the first kind). *Let  $u_h^{dG}$  and  $(\varepsilon_h, u_h)$ , be the solution of the discrete direct problems (2) and (12), respectively. Let  $v_h^{dG,*}$  and  $(v_h^*, w_h^*)$ , be the solution of the discrete adjoint problems (25) and (24), respectively. The following upper bound holds true:*

$$|q(u_h^{dG} - u_h)| \leq E(\varepsilon_h, v_h^{dG,*} - v_h^*). \quad (43)$$

Moreover, if either of the goal saturation assumptions is satisfied (i.e., Assumption 8 or 9), there exists a positive constant  $C > 0$ , such that:

$$|q(u - u_h)| \leq C E(\varepsilon_h, v_h^{dG,*} - v_h^*), \quad (44)$$

with  $u$  being the analytical solution of problem (1).

We introduce the following assumption:

**Assumption 11** (Local a posteriori adjoint residual estimation). *There exists a mesh independent positive constant  $C_{sta}^*$ , such that:*

$$\|v_h^{dG,*} - v_h\|_T \leq \frac{1}{C_{sta}^*} \|\varepsilon_h^*\|_T, \text{ for all } T \in \mathcal{P}_h. \quad (45)$$

Then, the following result is a direct consequence of Proposition 7:

**Proposition 8** (Upper bound of the second kind). *Consider the same hypotheses of Proposition 7. Let  $\varepsilon_h^*$  be the solution of the adjoint residual problem (28). If Assumption 11 is satisfied, it holds:*

$$|q(u_h^{dG} - u_h)| \leq \frac{1}{C_{sta}^*} E(\varepsilon_h, \varepsilon_h^*). \quad (46)$$

Moreover, if either of the goal saturation assumptions 8 or 9 is satisfied, there exists a positive constant  $C > 0$ , such that:

$$|q(u - u_h)| \leq C E(\varepsilon_h, \varepsilon_h^*). \quad (47)$$

with  $u$  being the analytical solution of problem (1).

Assumption 11 ensures the existence of a localizable a posteriori error estimate in line with (30).

**Remark 6** (Upper bound for the energy norm residual representative).  $E(\varepsilon_h, \varepsilon_h)$  is the square of the global error estimator considered in [12]. To compare our results with those of [12], we square the proportion of the total residual estimates employed in the Dörfler bulk-chasing criterion.

## 6. Model problem: A diffusion-advection-reaction problem

### 6.1. Continuous setting

Let  $\Omega \subset \mathbb{R}^d$ , with  $d = 2, 3$ , be an open and bounded Lipschitz domain with boundary  $\Gamma := \partial\Omega$ , and denote by  $\mathbf{n}$  its outward unit normal vector. Using the standard notation for Sobolev and Lebesgue spaces and their norms, let  $\kappa > 0$  be a diffusive coefficient in  $\Omega$ ,  $\mathbf{b} \in [W^{1,\infty}(\Omega)]^d$  be a divergence-free advective velocity field, and  $\gamma \geq 0$  be a reactive coefficient. As model problem, we consider the following diffusion-advection-reaction problem:

$$\begin{cases} \text{Find } u \text{ such that:} \\ -\operatorname{div}(\kappa \nabla u) + \mathbf{b} \cdot \nabla u + \gamma u = f, & \text{in } \Omega, \\ u = g_D, & \text{on } \Gamma, \end{cases} \quad (48)$$

where  $f \in L^2(\Omega)$  is a spatial source and  $g_D \in H^{1/2}(\Gamma)$  defines the boundary data. If  $g_D \equiv 0$ , the weak variational formulation of problem (48) reads:

$$\begin{cases} \text{Find } u \in U := V, \text{ such that,} \\ b(u, v) := \int_{\Omega} (\kappa \nabla u \cdot \nabla v - u(\mathbf{b} \cdot \nabla v) + \gamma u v) = l(v) := \int_{\Omega} f v, \quad \forall v \in V, \end{cases} \quad (49)$$

with energy space  $V := H_0^1(\Omega) = \{v \in H^1(\Omega) : v|_{\Gamma} = 0\}$ . Denoting by  $\|v\|_{\Omega}^2 = \int_{\Omega} v^2$  the standard  $L^2$ -norm, and considering the  $H^1$ -norm:

$$\|v\|_{1,\Omega}^2 := \|\nabla v\|_{\Omega}^2 + \|v\|_{\Omega}^2, \quad (50)$$

a straightforward verification shows that the bilinear form  $b(\cdot, \cdot)$  in (49) is bounded in  $V \times V$ , that is, there exists a constant  $M > 0$ , such that:

$$b(u, v) \leq M \|u\|_{1,\Omega} \|v\|_{1,\Omega}, \quad \forall u, v \in V. \quad (51)$$

This bilinear form is also coercive in  $V$ , that is, there exists a constant  $\alpha > 0$ , such that:

$$b(v, v) \geq \alpha \|v\|_{1,\Omega}^2, \quad \forall v \in V. \quad (52)$$

Since  $\mathbf{b}$  is divergence-free, it holds:

$$\int_{\Omega} w(\mathbf{b} \cdot \nabla v) = - \int_{\Omega} (\mathbf{b} \cdot \nabla w) v, \quad \forall w, v \in V, \quad (53)$$

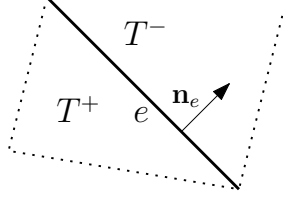


Figure 1: Skeleton orientation over the internal face  $e = \partial T^+ \cap \partial T^-$ .

and thus  $\int_{\Omega} v(\mathbf{b} \cdot \nabla v) = 0$ , for all  $v \in V$ . Therefore, well-posedness for the weak problem (60) is proved by evoking the Lax-Milgram theorem (cf., [29]). Finally, when  $g_D$  does not vanish in  $\Gamma$ , the weak variational formulation of problem (48) is equivalently obtained in terms of the auxiliary variable  $\tilde{u} := u - w_D$ , with  $w_D \in H^1(\Omega)$  a function satisfying  $w_D = g_D$  in  $H^{1/2}(\Gamma)$ . The existence of  $w_D$  is guaranteed as consequence of the surjectivity of the Dirichlet map from  $H^1(\Omega)$  to  $H^{1/2}(\Gamma)$ .

## 6.2. Discrete setting

Let  $\mathcal{P}_h$  be a conforming partition of the domain  $\Omega$  into open elements  $T \subset \Omega$ , such that:

$$\Omega_h := \bigcup_{T \in \mathcal{P}_h} T, \quad \text{satisfies} \quad \Omega = \text{int}(\overline{\Omega_h}). \quad (54)$$

For any  $T \in \mathcal{P}_h$ , we denote by  $h_T$  its diameter and by  $\partial T$  its boundary. Let  $\mathcal{S}_h^0$  be the set of interior edges/faces obtained from the intersection of two adjoint elements, as shown in Figure 1. Also,  $\mathcal{S}_h^\partial$  are the edges/faces that belong to the boundary  $\partial\Omega_h$ , and  $\mathcal{S}_h := \mathcal{S}_h^0 \cup \mathcal{S}_h^\partial$  form the skeleton of  $\Omega_h$ . For  $k \geq 1$ , we define the following standard broken Hilbert spaces over  $\Omega_h$ :

$$H^k(\Omega_h) := \left\{ v \in L^2(\Omega) : v \in H^k(T), \forall T \in \mathcal{P}_h \right\}. \quad (55)$$

For any  $v_h \in H^1(\Omega_h)$ , we define the jump function  $\llbracket v_h \rrbracket(\mathbf{x})$  and the average function  $\{v_h\}(\mathbf{x})$  respectively, restricted to an interior face/edge  $e = \partial K^+ \cap \partial K^- \in \mathcal{S}_h^0$ , as:

$$\llbracket v_h \rrbracket(\mathbf{x})|_e := v_h^+(\mathbf{x}) - v_h^-(\mathbf{x}), \quad \{v_h\}(\mathbf{x})|_e := \frac{1}{2}(v_h^+(\mathbf{x}) + v_h^-(\mathbf{x})), \quad \forall e \in \mathcal{S}_h^0, \quad (56)$$

where  $v_h^+$ ,  $v_h^-$  denote the traces over  $e = \partial T^+ \cap \partial T^-$  with respect to a predefined normal  $\mathbf{n}_e$ , as shown in Figure 1. We extend the definitions of (56) to  $e \in \mathcal{S}_h^\partial$  by setting:

$$\mathbf{n}_e(\mathbf{x}) := \mathbf{n}(\mathbf{x}), \quad \llbracket v_h \rrbracket(\mathbf{x})|_e := \{v_h\}(\mathbf{x})|_e := v_h(\mathbf{x})|_e \quad \forall e \in \mathcal{S}_h^\partial, \quad (57)$$

where  $\mathbf{n}$  denotes the outward normal to  $\partial\Omega$ . Let  $\mathbb{P}^p(T)$  be the set of polynomials of degree  $p \geq 1$  over the element  $T$ . We consider the following broken polynomial space:

$$\mathbb{P}^p(\Omega_h) := \left\{ v \in L^2(\Omega) : v|_T \in \mathbb{P}^p(T), \forall T \in \mathcal{P}_h \right\}. \quad (58)$$

For a given  $p \geq 1$ , we denote by  $V_h := \mathbb{P}^p(\Omega_h)$  endowed with a discrete norm  $\|\cdot\|_{V_h}$ .



### 6.3. DG variational formulations

In this section, we briefly introduce two possible consistent dG formulations (in primal form) for diffusion-advection-reaction problems. We analyze their inf-sup stability in terms of a discrete norm we generalize from [4, 22, 42]. For detailed discussions of dG schemes for elliptic problems, see for instance [3, 21, 42].

For a given  $p \geq 1$  and  $\epsilon = \pm 1$ , we use a dG direct problem (2) with the discrete linear operator  $l_h(\cdot)$ , and bilinear operator  $b_h(\cdot, \cdot)$  defined as:

$$l_h(v_h) = \sum_{T \in \mathcal{T}_h} \int_T f v_h + \sum_{e \in \mathcal{E}_h^\partial} \left( \epsilon \int_e g_D \kappa \nabla v_h \cdot n_e + \int_e (\mathbf{b} \cdot \mathbf{n}_e)^\ominus g_D v_h \right), \quad (59)$$

and

$$b_h(w_h, v_h) := b_h^\epsilon(w_h, v_h) + b_h^{\text{up}}(w_h, v_h), \quad (60)$$

with

$$\begin{aligned} b_h^\epsilon(w_h, v_h) := & \sum_{T \in \mathcal{T}_h} \int_T \kappa \nabla w_h \nabla v_h + \sum_{e \in \mathcal{E}_h} \kappa \frac{\eta_\epsilon}{h_e} \int_e \llbracket w_h \rrbracket \llbracket v_h \rrbracket \\ & - \sum_{e \in \mathcal{E}_h} \int_e \{ \kappa \nabla w_h \} \cdot n_e \llbracket v_h \rrbracket + \epsilon \int_e \llbracket w_h \rrbracket \{ \kappa \nabla v_h \} \cdot n_e, \end{aligned} \quad (61)$$

$$\begin{aligned} b_h^{\text{up}}(w_h, v_h) := & \sum_{T \in \mathcal{T}_h} \int_T (\mathbf{b} \cdot \nabla w_h + \gamma w_h) v_h + \sum_{e \in \mathcal{E}_h^\partial} \int_e (\mathbf{b} \cdot \mathbf{n}_e)^\ominus w_h v_h \\ & - \sum_{e \in \mathcal{E}_h^0} \int_e (\mathbf{b} \cdot \mathbf{n}_e) \llbracket w_h \rrbracket \{ v_h \} + \frac{\eta_u}{2} \sum_{e \in \mathcal{E}_h^0} \int_e |\mathbf{b} \cdot \mathbf{n}_e| \llbracket w_h \rrbracket \llbracket v_h \rrbracket. \end{aligned} \quad (62)$$

Here  $\eta_\epsilon, \eta_u > 0$  are user-defined stabilization parameters,  $x^\ominus = \frac{1}{2}(|x| - x)$  denotes the negative part of  $x$  (a positive-valued function), and

$$h_e := \begin{cases} \frac{1}{2}(h_{T^+} + h_{T^-}), & \text{if } e = \partial T^+ \cap \partial T^-, \\ h_T, & \text{if } e = \partial T \cap \partial \Omega_h. \end{cases} \quad (63)$$

**Remark 7** (Advection-dominated case). *When  $\kappa \ll \|\mathbf{b}\|_{\infty, \Omega}$ , the bilinear form  $b_h$  behaves as the bilinear form  $b_h^{\text{up}}$ . Thus, the discrete solution is close to the discrete approximation of the following continuous problem:*

$$\begin{cases} \text{Find } u \text{ such that:} \\ \mathbf{b} \cdot \nabla u + \gamma u = f, & \text{in } \Omega, \\ u = g^-, & \text{on } \Gamma^-, \end{cases} \quad (64)$$

where  $\Gamma^- := \{\mathbf{x} \in \Gamma : \mathbf{b}(\mathbf{x}) \cdot n(\mathbf{x}) < 0\}$  is the inflow boundary of  $\Omega$  and  $g^- = g_D|_{\Gamma^-}$  is the Dirichlet boundary data restricted to  $\Gamma^-$  with  $(\mathbf{b} \cdot \mathbf{n})^\ominus \neq 0$  on  $\Gamma^-$  only.

The discrete formulation couples two independent inf-sup stable schemes. First, the upwind scheme (up) handles the advective-reactive part of the equation (see [11]

and Remark 7). Second, an  $\epsilon$ -dependent formulation encompasses two alternative schemes for the diffusive part: a) the Symmetric Interior Penalization (SIP) when  $\epsilon = -1$  (see [2]) and b) the Non-symmetric Interior Penalization (NIP) when  $\epsilon = 1$  (see [43]). We consider these two particular formulations since the resulting scheme is consistent for  $\kappa > 0$  provided  $u \in H^2(\Omega)$ . However, the only one being also adjoint consistent is the one with  $\epsilon = -1$ , since the NIP formulation is not adjoint consistent (cf., [3]).

**Remark 8** (Generalizations). *We assume  $\kappa$  to be constant, and  $\mathbf{b}$  to be a divergence-free velocity field, and the solution  $u$  to satisfy Dirichlet boundary conditions to simplify the discussion. The use of heterogeneous and non-isotropic diffusive terms, non-solenoidal advective fields, and non-homogeneous Robin-type boundary conditions require slight modifications of the bilinear and linear forms [21].*

### 6.3.1. $V_h$ -norm, inf-sup stability, and boundedness

For the discrete space  $V_h$ , we consider the following induced norm:

$$\|\cdot\|_{V_h}^2 = (\cdot, \cdot)_{V_h} := (\cdot, \cdot)_\epsilon + (\cdot, \cdot)_{\text{up}}, \quad (65)$$

where, for any  $w_h, v_h \in V_h$ , we define:

$$(w_h, v_h)_\epsilon := \sum_{T \in \mathcal{T}_h} \kappa \int_T \nabla w_h \cdot \nabla v_h + \sum_{e \in \mathcal{S}_h} \kappa \frac{\eta_\epsilon}{h_e} \int_e \llbracket w_h \rrbracket \llbracket v_h \rrbracket, \quad (66)$$

$$\begin{aligned} (w_h, v_h)_{\text{up}} := & \sum_{T \in \mathcal{T}_h} \int_T (\gamma + \beta L^{-1}) w_h v_h + \beta_l \sum_{T \in \mathcal{T}_h} h_T \int_T (\mathbf{b} \cdot \nabla w_h) (\mathbf{b} \cdot \nabla v_h) \\ & + \sum_{e \in \mathcal{S}_h^\partial} \frac{1}{2} \int_e |\mathbf{b} \cdot \mathbf{n}_e| w_h v_h + \sum_{e \in \mathcal{S}_h^0} \frac{\eta_u}{2} \int_e |\mathbf{b} \cdot \mathbf{n}_e| \llbracket w_h \rrbracket \llbracket v_h \rrbracket, \end{aligned} \quad (67)$$

with  $\beta := \|\mathbf{b}\|_{[L^\infty(\Omega)]^d}$ ,  $L$  the diameter of the domain  $\Omega$  (i.e., the diameter of the largest circumference contained in  $\Omega$ ), and  $\beta_l$  defined as:

$$\beta_l := \begin{cases} \beta^{-1}, & \text{if } \beta > 0, \\ 0, & \text{if } \beta = 0. \end{cases} \quad (68)$$

**Remark 9** (Vanishing advection consistency). *The norm definition (65) is consistent in the limit case  $\beta \rightarrow 0^+$  since, for all  $v_h \in V_h$ , it holds:*

$$\beta_l \sum_{T \in \mathcal{T}_h} h_T \int_T (\mathbf{b} \cdot \nabla v_h)^2 \leq \beta_l \beta^2 \sum_{T \in \mathcal{T}_h} h_T \int_T |\nabla v_h|^2 \rightarrow 0^+, \text{ when } \beta \rightarrow 0^+.$$

Before delving into the proof of the inf-sup stability of the formulations, we recall the sufficient conditions to ensure the coercivity of bilinear forms [42]:

**Lemma 1** (Coercivity for pure diffusion). *Consider the bilinear form  $b_\epsilon(\cdot, \cdot)$  of (61), and assume that one of the following cases holds true:*

- i) NIP:  $\epsilon = 1$ ,  $p \geq 1$  and  $\eta_{-1} > 0$  for all  $e \in \mathcal{S}_h$ .

ii) SIP:  $\epsilon = -1$ ,  $p \geq 1$  and  $\eta_1$  is bounded below by a sufficiently large constant for all  $e \in \mathcal{S}_h$ .

Then, the bilinear form  $b_\epsilon(\cdot, \cdot)$  is coercive in  $V_h$  with respect to the norm  $\|\cdot\|_\epsilon^2 := (\cdot, \cdot)_\epsilon$  (cf., (52)), where the stability constant

$$C_{sta} = \begin{cases} 1 & \text{for } \epsilon = +1, \\ \frac{1}{2} & \text{for } \epsilon = -1. \end{cases}$$

Combining this result with a slight variation of the arguments in [21, Chap. 4.6.3], the following results are proved:

**Lemma 2** (Inf-sup stability). *In the above framework, consider  $\epsilon \in \{-1, 1\}$ ,  $p \geq 1$  and  $\eta_\epsilon \geq 0$  satisfying either case in Lemma 1. Then, Assumption 1 is satisfied.*

**Lemma 3** (Boundedness). *Under the same hypotheses of Lemma 2, Assumption 3 is satisfied with the following extended norm of  $V_h$ :*

$$\|v\|_{V_{h,\#}}^2 := \|v\|_{V_h}^2 + \beta \sum_{T \in \mathcal{T}_h} \int_T v^2 + \sum_{T \in \mathcal{T}_h} h_T \int_{\partial T} \kappa (\nabla v \cdot \mathbf{n}_T)^2. \quad (69)$$

**Remark 10** (Norm modification). *The discrete norm (65) is a slight modification of the norm in [4] such that it does depend on  $\eta_\epsilon$ . We modify the norm because it plays a fundamental role in the stabilization of the method [12]. In particular, the discrete norm (65) lets us tune  $\eta_\epsilon > 0$  to improve the discrete solution while keeping the stability constant unchanged. This is not the case for the  $\eta_\epsilon$ -independent norm (see [22, Lemma 4.12]).*

**Remark 11** (Localization of the inner product). *We localize the inner product (65) satisfying Assumption 10 as:*

$$(w_h, v_h)_{V_h} = (w_h, v_h)_T := (w_h, v_h)_{loc,T} + \frac{1}{2} \sum_{e \in \mathcal{S}_h^0 \cap \partial T} S_e(w_h, v_h),$$

with

$$\begin{aligned} (w_h, v_h)_{loc,T} &:= \kappa \int_T \nabla w_h \cdot \nabla v_h + \int_T (\gamma + \beta L^{-1}) w_h v_h + \beta_l h_T \int_T (\mathbf{b} \cdot \nabla w_h) (\mathbf{b} \cdot \nabla v_h) \\ &\quad + \sum_{e \in \mathcal{S}_h^0 \cap \partial T} \int_e \left( \kappa \frac{\eta_\epsilon}{h_e} + \frac{1}{2} |\mathbf{b} \cdot \mathbf{n}_e| \right) w_h v_h, \\ S_e(w_h, v_h) &:= \int_e \left( \kappa \frac{\eta_\epsilon}{h_e} + \frac{\eta_u}{2} |\mathbf{b} \cdot \mathbf{n}_e| \right) [w_h] [v_h]. \end{aligned}$$

## 7. Numerical examples

We consider several test cases focusing on diffusion-advection-reaction problems. These examples demonstrate the performance of the four-steps GoA methodology of Section 4. We use FEniCS [1] to perform the simulations and we perform

the GoA following the same setting. We consider a QoI of the form:

$$q(u) = \frac{1}{|\Omega_0|} \int_{\Omega_0} u, \quad (70)$$

where  $u$  denotes the analytic solution of the corresponding problem, and  $\Omega_0$  is a subdomain of the physical domain  $\Omega$ .

For a given polynomial degree  $p \geq 1$ , we consider the test space  $V_h$  to be a standard discontinuous piece-wise polynomial space of degree  $p$ , and the trial space  $U_h$  as a standard FEM subspace of continuous piece-wise polynomial functions of degree  $p$  (i.e.,  $H^1$ -conforming). We set the diffusive stabilization parameter to  $\eta_s = 3(p+1)(p+2)$ , and the advective stabilization parameter to  $\eta_u = p$ .

The initial mesh is  $\Omega_0$ -conforming. We then perform a loop following the standard modules in adaptive procedures:

$$\text{SOLVE} \rightarrow \text{ESTIMATE} \rightarrow \text{MARK} \rightarrow \text{REFINE}.$$

The estimation procedure considers independent adaptive mesh refinements based on the following error estimates (see Section 5.1):

1.  $E(\varepsilon_h, \varepsilon_h)$ : Energy norm-based error estimate (see Remark 6).
2.  $E(\varepsilon_h, \varepsilon_h^*)$ : GoA error estimate depending implicitly of the dG solutions.
3.  $E(\varepsilon_h, v_h^{\text{dG},*} - v_h^*)$ : GoA error estimate depending explicitly of the adjoint dG solution  $v_h^{\text{dG},*}$ .

The marking procedure follows the Dörfler bulk-chasing criterion with the corresponding fraction to be 25% (see Remark 6). Finally, we employ a bisection-type refinement criterion [6]. In the first two examples, we use  $LU$  direct solver. In the last example, we use an iterative scheme (see [12]) on the resulting multiple right hand sides. We then postprocess error estimate  $\varepsilon_h^*$  by solving (28) using a preconditioned conjugate gradient method. In this last step, we use the same preconditioner for the iterative solver.

### 7.1. Advection-reaction problem

As a first example, we consider the advection-reaction problem (64) in the unit square  $\Omega = (0, 1)^2 \subset \mathbb{R}^2$ , with a constant velocity field  $\mathbf{b} = (3, 1)^T$ . For a given  $\gamma \geq 0$ , the source term is  $f = \gamma u$  in  $\Omega$ , and an inflow boundary datum  $g^- = u|_{\Gamma^-}$ , where  $\Gamma^- = \{(0, y), y \in (0, 1)\} \cup \{(x, 0), x \in (0, 1)\}$ , and the exact solution  $u$  is (see Figure 2a):

$$u(x_1, x_2) = 2 + \tanh\left(10\left(x_2 - \frac{x_1}{3} - \frac{1}{4}\right)\right) + \tanh\left(1000\left(x_2 - \frac{x_1}{3} - \frac{3}{4}\right)\right). \quad (71)$$

Since  $\kappa = 0$ , the dG bilinear and linear forms correspond to equations (59) and (60), respectively, while the discrete inner product corresponds to equation (65).

The nature of the analytical solution  $u$  implies that an adaptivity based on the energy norm refines in a neighbourhood of the characteristic line starting from the inflow boundary in  $y = 3/4$  (cf. [12]). We analyze a pure advection case ( $\gamma = 0$ ), and

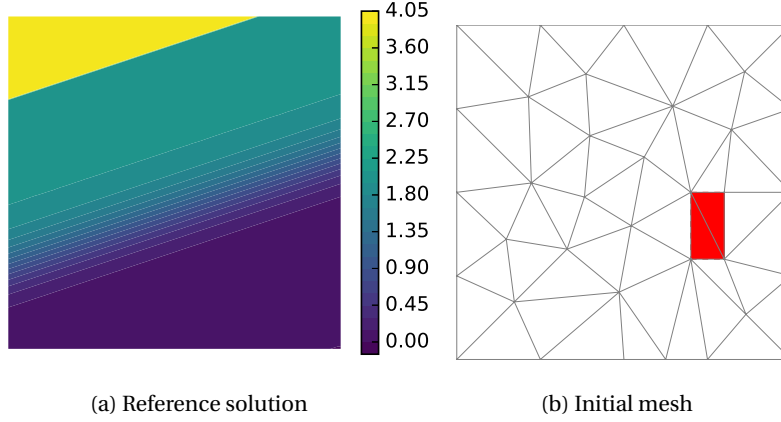


Figure 2: Reference solution and initial mesh

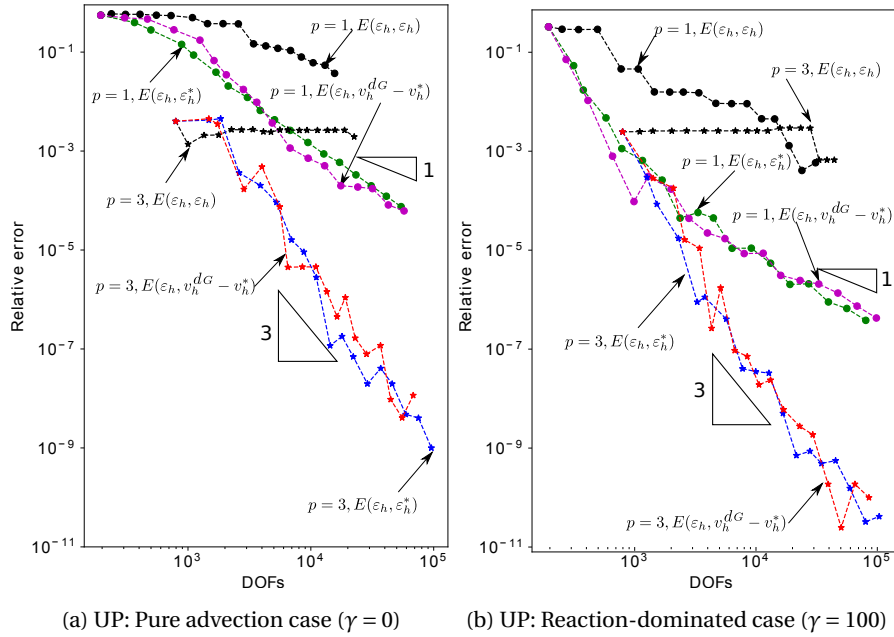


Figure 3: Relative error ( $|q(u - u_h)|/|q(u)|$ ) in quantity of interest (QoI) using upwinded (UP) scheme for (a) pure advection and (b) reaction-dominated problems. (See Section 5.1 for a detailed discussion.)

a reaction-dominated case ( $\gamma = 100$ ). We set  $\Omega_0 = (0.7, 0.8) \times (0.3, 0.5)$  as the subdomain that defines the QoI, and we consider the  $\Omega_0$ -conforming mesh of Figure 2b as our starting point for the adaptive procedure.

Figure 3a shows the relative error for the pure advection case for three estimators. We consider two polynomial orders (i.e.,  $p = 1, 3$ ) and plot the evolution of the relative error  $|q(u - u_h)|/|q(u)|$  versus the total number of degrees of freedom

in the system (DOFs) we use to solve the saddle-point problem (12) (i.e.  $\dim(V_h) + \dim(U_h)$ ). In Figure 3b, we repeat these plots for the reactive dominant case. These figures show up to eighteen levels of refinement. As our theoretical analysis predicts, the convergence rates of the GoA error estimates  $E(\varepsilon_h, \varepsilon_h^*)$  and  $E(\varepsilon_h, v_h^{dG,*} - v_h^*)$  are significantly better than those the energy norm delivers. Moreover, both GoA error estimates we propose deliver similar convergence rates.

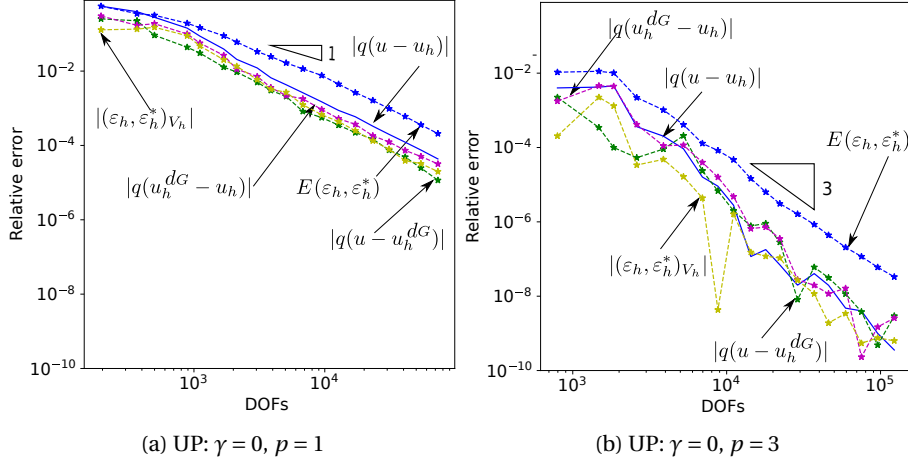


Figure 4: Discrete relative error for upwinded (UP) scheme for pure advection,  $\gamma = 0$ : goal-oriented error estimate  $E(\varepsilon_h, \varepsilon_h^*)$  (see Section 5.1 for definitions).

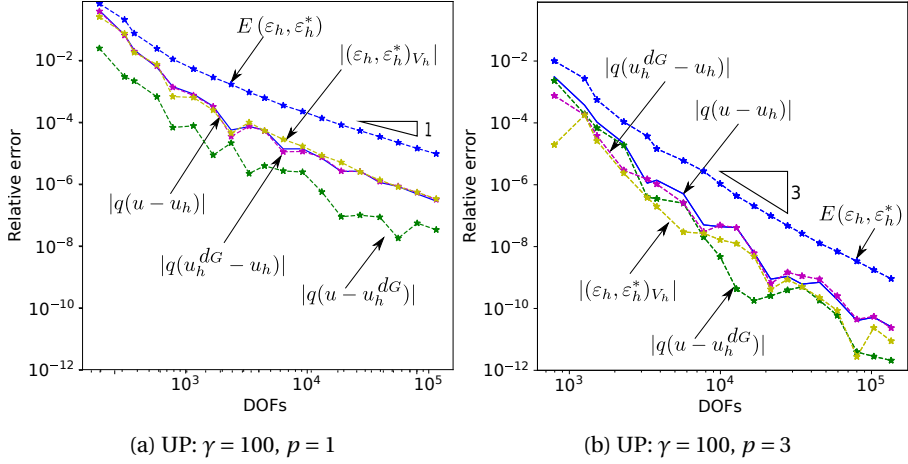


Figure 5: Discrete relative error for upwinded (UP) scheme for reaction-dominated case,  $\gamma = 100$ : goal-oriented error estimate  $E(\varepsilon_h, \varepsilon_h^*)$  (see Section 5.1 for definitions).

Figure 4 displays the evolution of the quantities  $|q(u - u_h)|$ ,  $|q(u - u_h^{dG})|$ ,  $|q(u_h^{dG} - u_h)|$ ,  $|(\varepsilon_h, \varepsilon_h^*)_{V_h}|$  (scaled by  $|q(u)|$ ) against the total number of DOFs. Each subfigure

displays for the pure advection case ( $\gamma = 0$ ) the behaviour for polynomial degrees  $p = 1$  (a), and  $p = 3$  (b). Similarly, Figure 5 displays the same ratios for the reaction dominated case ( $\gamma = 100$ ). These figures show that all the quantities share the same upper bound. Moreover, Figures 4a, 5a and 5b show that the curve  $|q(u - u_h^{\text{dG}})|$  remains below the curve  $|q(u - u_h)|$ . This bound implies that the Goal saturation Assumption 8 is satisfied. While for pure advection ( $\gamma = 0$ ) with polynomial order  $p = 3$  (see Figure 4b) this assumption is violated. Nevertheless, the weaker Assumption 9 is satisfied instead.

Figure 6 displays the resulting meshes at the thirteenth level of refinement using the energy error estimate (i.e.,  $E(\varepsilon_h, \varepsilon_h)$ ) for pure advection (a), and reaction-dominated (b) cases. Similarly, Figure 7 displays the meshes when using the estimate  $E(\varepsilon_h, \varepsilon_h^*)$ . A comparison of these figures shows that the GoA estimates adjust the mesh refinement process according to the physical nature of the problem. In both cases, the energy error estimates attenuate the characteristic line that starts at  $\gamma = 3/4$  and induces an interior layer.

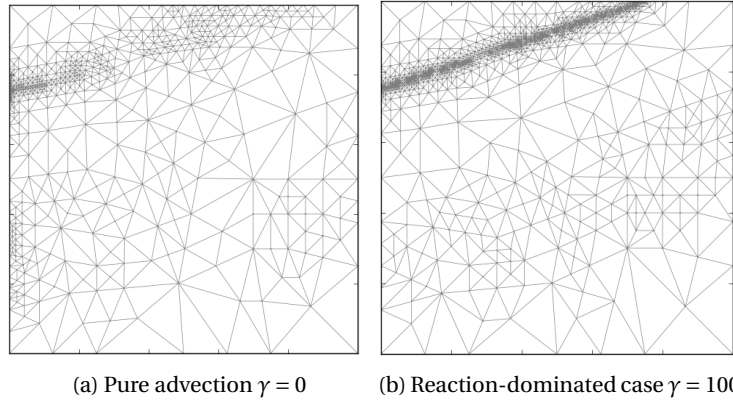


Figure 6: Comparison of resulting mesh at thirteenth level of refinement using the UP scheme with  $p = 1$  and the energy-based error estimate  $E(\varepsilon_h, \varepsilon_h)$  (see Section 5.1 for definitions).

## 7.2. Diffusion problem

Now, we solve the diffusion problem in an L-shape domain  $\Omega := (-5, 40)^2 \setminus (-5, 0)^2$ :

$$\begin{cases} \text{Find } u \text{ such that:} \\ -\Delta u = 0, & \text{in } \Omega, \\ u = u_D, & \text{on } \partial\Omega, \end{cases} \quad (72)$$

where  $u_D$  denotes the Dirichlet trace of the following harmonic function (see Fig. 8a):

$$u(r, \theta) := r^{\frac{2}{3}} \sin\left(\frac{2}{3}(\pi - \theta)\right), \text{ with } -\pi < \theta \leq \pi, \text{ and } r > 0. \quad (73)$$

Equations (59) and (60) express the corresponding dG bilinear and linear forms, respectively, while (65) defines the discrete inner product with  $\kappa = 1$ ,  $f = 0$ ,  $\mathbf{b} = \mathbf{0}$ ,

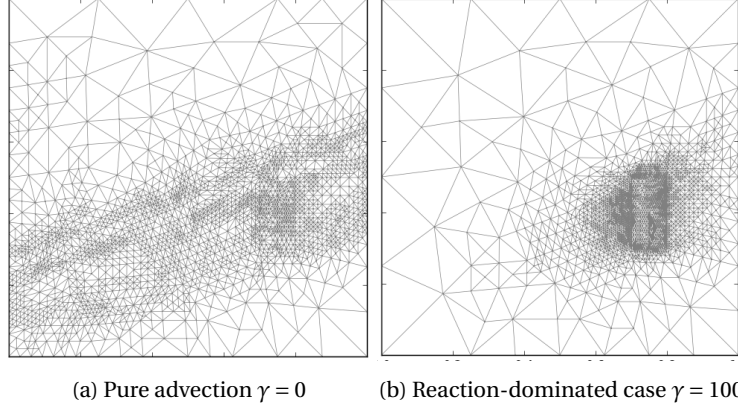


Figure 7: Comparison of resulting mesh at thirteenth level of refinement using the UP scheme with  $p = 1$  and the goal-oriented error estimate  $E(\varepsilon_h, \varepsilon_h^*)$  (see Section 5.1 for definitions).

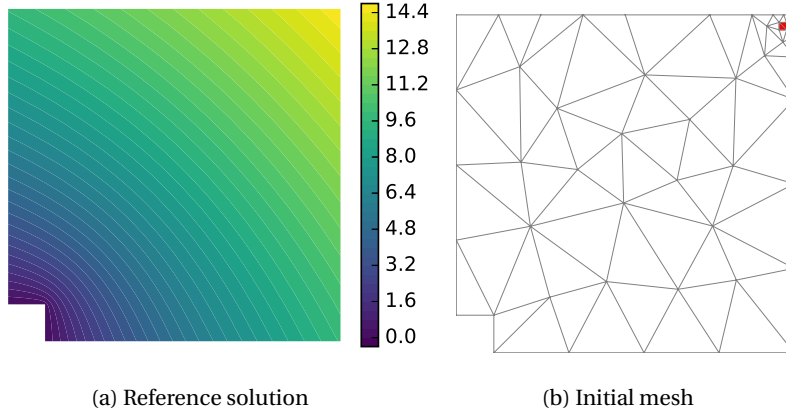


Figure 8: Reference solution and initial mesh

and  $\gamma = 0$ . Our description allows for two possible formulations: the Symmetric Interior Penalty (SIP) formulation ( $\epsilon = -1$ ) satisfying the adjoint Assumption 2, and the Nonsymmetric Interior Penalty (NIP) formulation ( $\epsilon = 1$ ), which does not satisfy this assumption.

To illustrate the effect of the GoA procedure, we consider the QoI defined over the subdomain  $\Omega_0 = (38, 39)^2$ , and the initial mesh shown in Figure 8b. The re-entrant corner introduces a singularity at the origin as  $u \in H^{5/3-\delta}(\Omega)$ , with  $\delta > 0$  [23]. Thus, an adaptive energy norm-based strategy enforces heavy refinements in a neighbourhood of the re-entrant corner, as Figure 9a shows. The figure shows the resulting mesh at refinement level 16 for the SIP scheme, with  $p = 1$ , using the global error estimator  $E(\varepsilon_h, \varepsilon_h)$ , and the same initial mesh.

We repeat the experiments of the previous section with polynomial degrees  $p = 1, 3$ . The GoA estimates reduce the refinements near the re-entrant corner (see Fig-



ure 9b). The figure shows the resulting mesh at refinement level 9 for the SIP formulation. As above, we start from Figure 8b and use the GoA estimate that  $E(\varepsilon_h, \varepsilon_h^*)$  produces.

Figures 10a and 10b display the relative error in the QoI ( $|q(u - u_h)|/|q(u)|$ ) versus the total number of DOFs (for the first 18 levels of refinement) using the SIP and NIP formulations, respectively. We consider polynomial degrees  $p = 1, 3$ , and the three possible error estimates. As in the previous example, the GoA error estimates deliver a clear improvement in the convergence rate when compared against the energy estimate. Additionally, the two GoA error estimates produce similar convergence rates for both SIP and NIP formulations. The robustness of the error estimation with respect to the discrete formulation shows that our GoA algorithm is independent of the adjoint Assumption 7.

Finally, Figure 11a compares several of the discrete quantities and validates the analysis we present in Section 5. The figure shows the first 18 levels of refinement estimating the error with  $E(\varepsilon_h, \varepsilon_h^*)$  for the SIP formulation with polynomial degree  $p = 1$ . In the figure, the  $|q(u - u_h^{\text{dG}})|$  remains below the curve  $|q(u - u_h)|$ , implying that the Assumption 8 is satisfied again. Moreover, the quantities  $|q(u - u_h)|$ ,  $|q(u - u_h^{\text{dG}})|$  and  $|\varepsilon_h, \varepsilon_h^*)|$  have the same rate of convergence. Interestingly, the convergence rate of the upper bound  $E(\varepsilon_h, \varepsilon_h^*)$  is lower than the one of the other curves. This allows us to speculate that the upper bound can be tightened. Nevertheless, this behaviour is independent of the GoA estimate as Figure 11b shows the behaviour of the error estimate  $E(\varepsilon_h, v_h^{\text{dG},*} - v_h^*)$ . Again, this result is in agreement with the a posteriori error analysis of Section 5, where we prove that  $E(\varepsilon_h, \varepsilon_h^*)$  and  $E(\varepsilon_h, v_h^{\text{dG},*} - v_h^*)$  are upper bounds only.

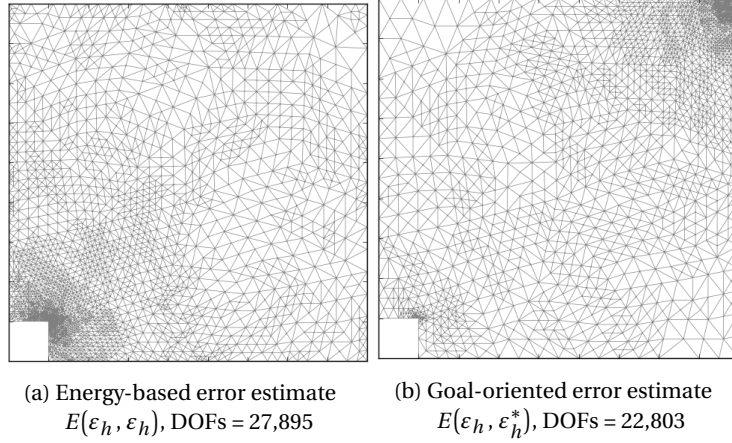


Figure 9: Comparison of resulting mesh for a comparable number of degrees of freedom (DOFs) using Symmetric Interior Penalty (SIP) with  $p = 1$ .

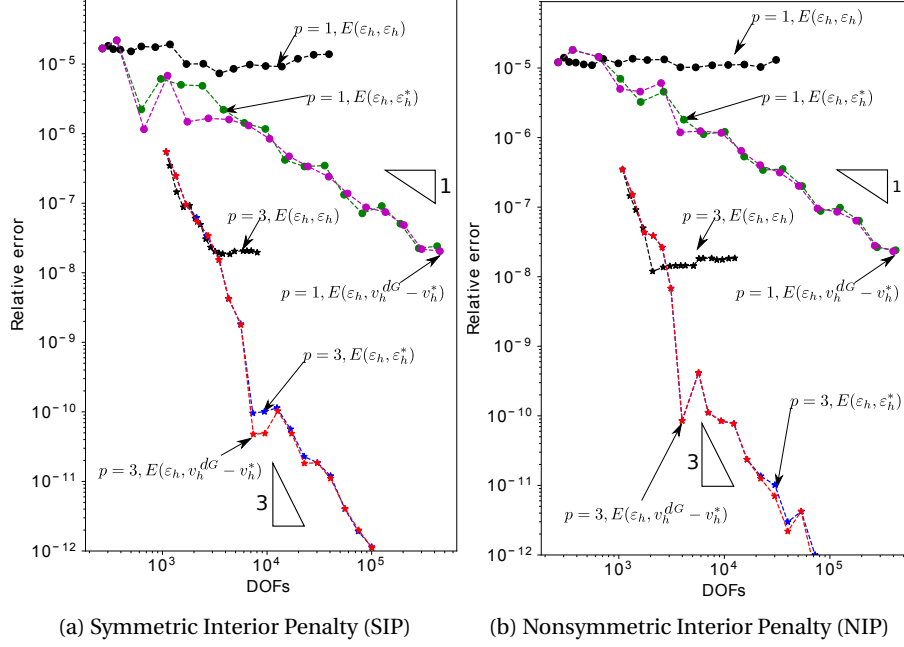


Figure 10: Relative error comparison in the quantity of interest (QoI) using the Symmetric Interior Penalty (SIP) and Nonsymmetric Interior Penalty (NIP) schemes for  $p = 1$ .

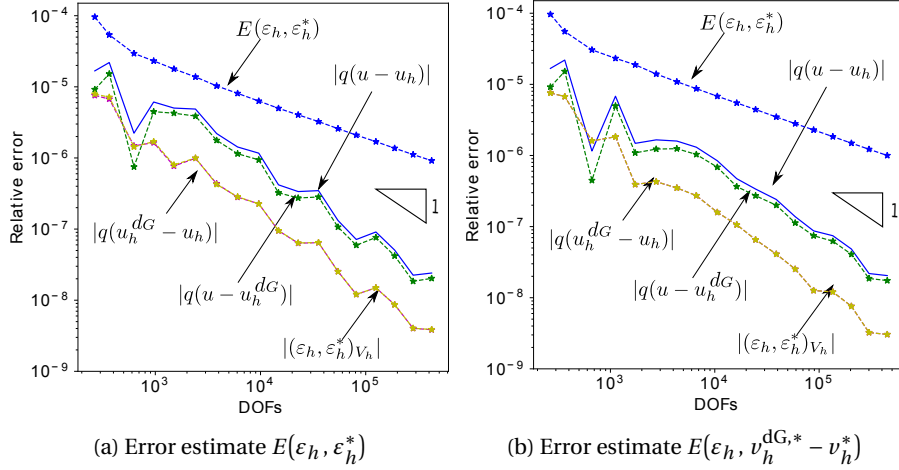


Figure 11: Comparison of goal-oriented error estimates for the Symmetric Interior Penalty (SIP),  $p = 1$ .

### 7.3. Advection-diffusion-reaction problem with dominant advection

As a final example, we consider a 3D advection-dominated diffusion-advection-reaction problem. We particularize the definition of problem (48). We denote by  $\mathbf{x} = (x_1, x_2, x_3)$  the space variable, and set the physical domain to the unit cube  $\Omega =$

$(0, 1)^3$ . We set  $f = 0$  as the source term,  $\kappa = 10^{-6}$  as the diffusive term,  $\mathbf{b} = (-0.6 \sin(6\pi x_3), 0.6 \cos(6\pi x_3), 1)$  as the velocity field, and  $\gamma = 10^{-6}$  as the reactive term. We also define the Dirichlet datum as

$$u_D = \begin{cases} 2 + \tanh(1000 c(0.1, (0.3, 0.3))) + \tanh(1000 c(0.1, (0.6, 0.6))), & \text{if } x_3 = 0, \\ 0, & \text{elsewhere,} \end{cases}$$

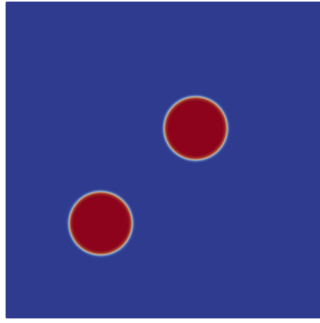
where  $c(r, (y_1, y_2)) := r^2 - (x_1 - y_1)^2 - (x_2 - y_2)^2$ . Here, the boundary datum  $u_D|_{x_3=0}$  corresponds to a smooth extension of a boundary source term which is different from zero in the interior of two circumferences, as shown in Figure 12a. The solution of this problem is close to the solution of a homogeneous pure advection problem (64) (i.e, with  $\gamma = 0$  and  $f = 0$ ) considering the inflow datum  $g^- = u_D|_{\Gamma^-}$ . Such solution corresponds to two smoothed spirals starting at  $x_3 = 0$ , and arriving to  $x_3 = 1$  (at the same starting position in the XY plane) after three periods of rotation (cf. [12]). However, the homogeneous outflow boundary condition at  $x_3 = 1$  induces strong boundary layers in the solution of the diffusive problem. Thus, this double spiral solution has strong interior and boundary layers.

As in the previous examples, the energy-based adaptivity refines the solution to minimize its global error. In this particular problem, the energy estimate first refines around the inflow region,  $x_3 = 0$  and then follows the velocity field  $\mathbf{b}$  towards the outflow region  $x_3 = 1$ . Figure 13a shows a solution contour for the eleventh level of refinement for a polynomial degree 1 and the initial mesh of Figure 12b. The error estimate in this case reads  $E(\varepsilon_h, \varepsilon_h)$ .

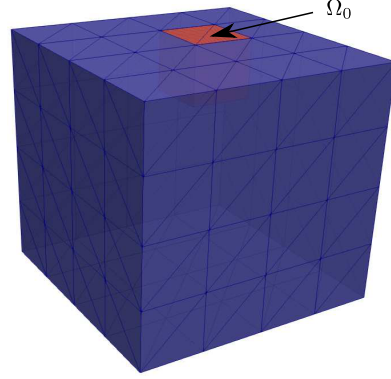
We measure the quantity of interest (QoI) in the cube  $\Omega_0 = (0.5, 0.75)^2 \times (0.75, 1)$  as the domain for the QoI. The domain  $\Omega_0$  only intersects the circumference with center  $(0.6, 0.6)$  and radius 0.1. Figure 13b shows the solution contours at its seventh level of refinement guided by the GoA error estimate  $E(\varepsilon_h, \varepsilon_h^*)$ . The problem setup is identical to the one described above. The goal-oriented strategy focuses on the refinement of the spiral, starting at the circumference of center  $(0.6, 0.6)$ . Additionally, the GoA strategy notoriously reduces refinements near the outflow boundary of both spirals. Figure 14 shows the relative error against the number of DOFs. We show the first nine levels of refinements for polynomial orders  $p = 1, 2$  for the energy-based (left), and the GoA (right) error estimates. Since the problem has no known analytical solution, we use an overkill simulation as a reference QoI. That is, we use the GoA strategy with polynomial degree  $p = 3$  for the discrete spaces. We use the value  $q(u_{ref}) \approx 0.28196$  as the reference QoI obtained after nine levels of GoA refinements, requiring a total of 1,528,018 DOFs to solve the final saddle-point problem. These figures show a significant error reduction in the QoI when comparing the results that the GoA estimates deliver against the energy-based ones.

## 8. Conclusions and further lines of work

In this paper, we present a new stabilized conforming goal-oriented adaptive method based on the stabilized finite element method introduced in [12]. The adaptive framework automatically delivers stable solutions for both the direct and adjoint problems. Our process requires the resolution of a third problem. This allows us

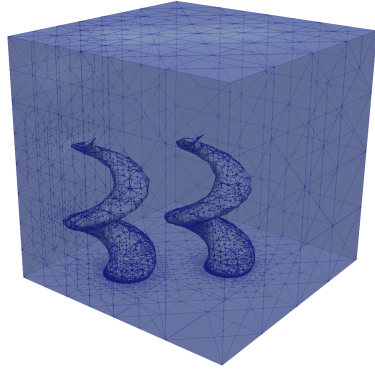


(a) Dirichlet boundary condition at  $x_3 = 0$

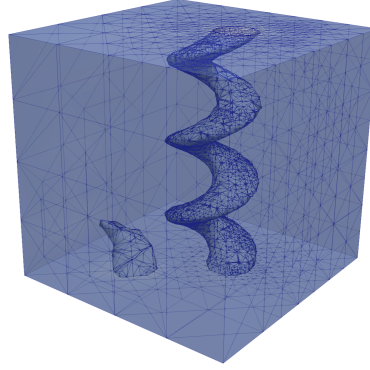


(b) Initial mesh

Figure 12: Boundary condition and initial mesh setup



(a) Energy-based error estimate  
 $E(\varepsilon_h, \varepsilon_h)$ , DOFs = 449,841



(b) Goal-oriented error estimate  
 $E(\varepsilon_h, \varepsilon_h^*)$ , DOFs = 313,704 DOFs

Figure 13: Resulting mesh contour comparison: Adaptivity driven by the energy-based  $E(\varepsilon_h, \varepsilon_h)$  (left) versus goal-oriented  $E(\varepsilon_h, \varepsilon_h^*)$  (right) error estimates.

to compute an error estimate for the quantity of interest robustly. We present two alternative definitions of the third problem. The first definition solves an adjoint discontinuous Galerkin formulation. The second one solves a discrete Riesz representation problem, which inverts a symmetric positive definite matrix using fast approximations. Under a meaningful assumption to be satisfied by the reference discontinuous Galerkin formulation, we prove that both definitions provide an upper bound for the error in the quantity of interest. We validate the superiority of our

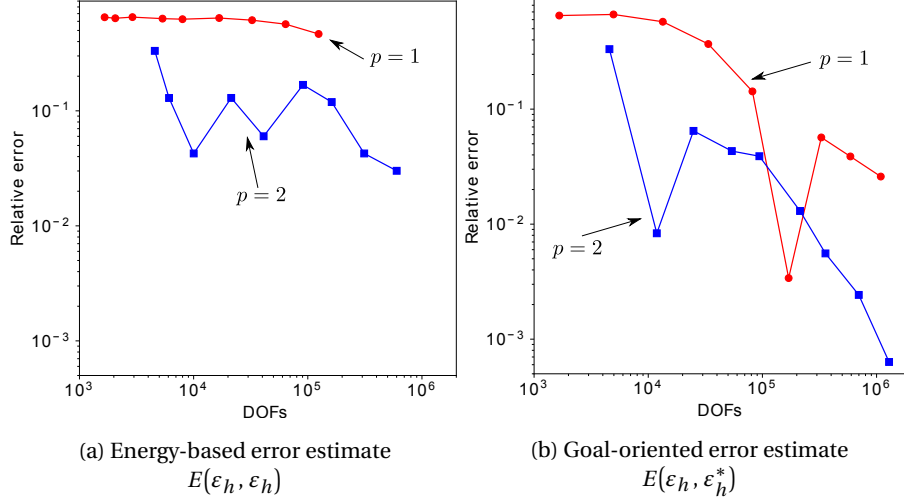


Figure 14: Relative error versus total number of degrees of freedom in the system (DOFs): Adaptivity driven by the energy-based  $E(\varepsilon_h, \varepsilon_h)$  (left) versus goal-oriented  $E(\varepsilon_h, \varepsilon_h^*)$  (right) error estimates. Data for nine levels of refinement, polynomial order  $p = 1, 2$ .

goal-oriented strategy against an energy-based error estimate numerically.

Further studies are on the way to explore the performance of the method when applied to other challenging problems. For example, we will study the performance of metal-air electrochemical cells to improve battery storage capacity. We are also pursuing the extension of the methodology to time-dependent problems by considering space-time formulations.

## Acknowledgements

This publication was made possible in part by the CSIRO Professorial Chair in Computational Geoscience at Curtin University and the Deep Earth Imaging Enterprise Future Science Platforms of the Commonwealth Scientific Industrial Research Organisation, CSIRO, of Australia. At Curtin University, The Curtin Corrosion Centre, the Curtin Institute for Computation, and The Institute for Geoscience Research (TIGeR) kindly provide continuing support. David Pardo has received funding from the European Union's Horizon 2020 research and innovation programme under the Marie Skłodowska-Curie grant agreement No 777778 (MATHROCKS), the European POCTEFA 2014-2020 Project PIXIL (EFA362/19) by the European Regional Development Fund (ERDF) through the Interreg V-A Spain-France-Andorra programme, the Project of the Spanish Ministry of Science and Innovation with reference PID2019-108111RB-I00 (FEDER/AEI), the BCAM "Severo Ochoa" accreditation of excellence (SEV-2017-0718), and the Basque Government through the BERC 2018-2021 program, the two Elkartek projects 3KIA (KK-2020/00049) and MATHEO (KK-2019-00085), the grant "Artificial Intelligence in BCAM number EXP. 2019/00432", and the Consolidated Research Group MATHMODE (IT1294-19) given by the Department of Ed-

ucation. Part of this work was carried over while the first author was invited by INRIA SERENA team in Paris.

## References

- [1] Alnæs, M. S., Blechta, J., Hake, J., Johansson, A., Kehlet, B., Logg, A., Richardson, C., Ring, J., Rognes, M. E., & Wells, G. N. (2015). The fenics project version 1.5. *Archive of Numerical Software*, 3, 9–23.
- [2] Arnold, D. N. (1982). An interior penalty finite element method with discontinuous elements. *SIAM journal on numerical analysis*, 19, 742–60.
- [3] Arnold, D. N., Brezzi, F., Cockburn, B., & Marini, L. D. (2002). Unified analysis of discontinuous galerkin methods for elliptic problems. *SIAM journal on numerical analysis*, 39, 1749–79.
- [4] Ayuso, B., & Marini, L. D. (2009). Discontinuous Galerkin methods for advection-diffusion-reaction problems. *SIAM J. Numer. Anal.*, 47, 1391–420.
- [5] Babuska, I., Zienkiewicz, O., Gago, J., & Oliveira, E. d. A. (1986). *Accuracy estimates and adaptive refinements in finite element computations*. John Wiley & Sons New York.
- [6] Bank, R. E., Sherman, A. H., & Weiser, A. (1983). Some refinement algorithms and data structures for regular local mesh refinement. *Scientific Computing, Applications of Mathematics and Computing to the Physical Sciences*, 1, 3–17.
- [7] Becker, R., & Rannacher, R. (1996). *Weighted a posteriori error control in FE methods*. IWR.
- [8] Boffi, D., Brezzi, F., Fortin, M. et al. (2013). *Mixed finite element methods and applications* volume 44. Springer.
- [9] Bramble, J. H., & Schatz, A. H. (1970). Rayleigh-Ritz-Galerkin-methods for Dirichlet’s problem using subspaces without boundary conditions. *Comm. Pure Appl. Math.*, 23, 653–75.
- [10] Brezzi, F., Marini, L. D., & Süli, E. (2004). Discontinuous Galerkin methods for first-order hyperbolic problems. *Math. Models Methods Appl. Sci.*, 14, 1893–903.
- [11] Brezzi, F., Marini, L. D., & Süli, E. (2004). Discontinuous galerkin methods for first-order hyperbolic problems. *Mathematical models and methods in applied sciences*, 14, 1893–903.
- [12] Calo, V. M., Ern, A., Muga, I., & Rojas, S. (2020). An adaptive stabilized conforming finite element method via residual minimization on dual discontinuous galerkin norms. *Computer Methods in Applied Mechanics and Engineering*, 363, 112891.

- [13] Chan, J., Heuer, N., Bui-Thanh, T., & Demkowicz, L. (2014). A robust DPG method for convection-dominated diffusion problems II: Adjoint boundary conditions and mesh-dependent test norms. *Comput. Math. Appl.*, 67, 771–95.
- [14] Cockburn, B., Karniadakis, G. E., & Shu, C.-W. (2000). *Discontinuous Galerkin Methods - Theory, Computation and Applications* volume 11 of *Lecture Notes in Computer Science and Engineering*. Springer.
- [15] Darrigrand, V., Rodríguez-Rozas, Á., Muga, I., Pardo, D., Romkes, A., & Prudhomme, S. (2018). Goal-oriented adaptivity using unconventional error representations for the multidimensional helmholtz equation. *International Journal for Numerical Methods in Engineering*, 113, 22–42.
- [16] Demkowicz, L., & Gopalakrishnan, J. (2010). A class of discontinuous Petrov–Galerkin methods. Part I: The transport equation. *Computer Methods in Applied Mechanics and Engineering*, 199, 1558–72.
- [17] Demkowicz, L., & Gopalakrishnan, J. (2011). A class of discontinuous Petrov–Galerkin methods. II. Optimal test functions. *Numerical Methods for Partial Differential Equations*, 27, 70–105.
- [18] Demkowicz, L., & Gopalakrishnan, J. (2014). An overview of the discontinuous Petrov Galerkin method. In X. Feng, O. Karakashian, & Y. Xing (Eds.), *Recent Developments in Discontinuous Galerkin Finite Element Methods for Partial Differential Equations: 2012 John H Barrett Memorial Lectures* (pp. 149–80). Cham: Springer volume 157 of *The IMA Volumes in Mathematics and its Applications*.
- [19] Demkowicz, L., Gopalakrishnan, J., & Niemi, A. H. (2012). A class of discontinuous Petrov–Galerkin methods. Part III: Adaptivity. *Applied numerical mathematics*, 62, 396–427.
- [20] Demkowicz, L., & Heuer, N. (2013). Robust DPG method for convection-dominated diffusion problems. *SIAM J. Numer. Anal.*, 51, 2514–37.
- [21] Di Pietro, D. A., & Ern, A. (2012). *Mathematical aspects of discontinuous Galerkin methods* volume 69. Springer Science.
- [22] Di Pietro, D. A., Ern, A., & Guermond, J.-L. (2008). Discontinuous galerkin methods for anisotropic semidefinite diffusion with advection. *SIAM Journal on Numerical Analysis*, 46, 805–31.
- [23] Dolejsi, V., Ern, A., & Vohralík, M. (2016). hp-adaptation driven by polynomial-degree-robust a posteriori error estimates for elliptic problems. *SIAM Journal on Scientific Computing*, 38, A3220–46.
- [24] Dörfler, W. (1996). A convergent adaptive algorithm for Poisson’s equation. *SIAM Journal on Numerical Analysis*, 33, 1106–24.

- [25] Džiškariani, A. (1968). The least square and Bubnov-Galerkin methods. *Ž. Vyčisl. Mat. i Mat. Fiz.*, 8, 1110–6.
- [26] Ern, A., & Guermond, J.-L. (2004). *Theory and practice of finite elements* volume 159. Springer Science.
- [27] Ern, A., & Guermond, J.-L. (2006). Discontinuous Galerkin Methods for Friedrichs' Systems. I. General theory. *SIAM Journal on Numerical Analysis*, 44, 753–78.
- [28] Ern, A., & Guermond, J.-L. (2016). Linear stabilization for first-order PDEs. In *Handbook of numerical methods for hyperbolic problems* (pp. 265–88). Elsevier/North-Holland, Amsterdam volume 17 of *Handb. Numer. Anal.*.
- [29] Evans, L. C. (2010). *Partial differential equations*. Providence, R.I.: American Mathematical Society.
- [30] Feischl, M., Praetorius, D., & Van der Zee, K. G. (2016). An abstract analysis of optimal goal-oriented adaptivity. *SIAM Journal on Numerical Analysis*, 54, 1423–48.
- [31] Hughes, T. J. R., Franca, L. P., & Hulbert, G. M. (1989). A new finite element formulation for computational fluid dynamics: VIII. The Galerkin/Least-Squares method for advection-diffusive equations. *Comput. Methods Appl. Mech. Engrg.*, 73, 173–89.
- [32] Hughes, T. J. R., Scovazzi, G., & Franca, L. P. (2017). Multiscale and Stabilized Methods. In *Encyclopedia of Computational Mechanics Second Edition* (pp. 1–64). American Cancer Society.
- [33] Jiang, B. (1998). *The Least-Squares Finite Element Method*. Springer.
- [34] Johnson, C., & Pitkäranta, J. (1986). An analysis of the discontinuous Galerkin method for a scalar hyperbolic equation. *Math. Comp.*, 46, 1–26.
- [35] Keith, B., Astaneh, A. V., & Demkowicz, L. F. (2019). Goal-oriented adaptive mesh refinement for discontinuous petrov–galerkin methods. *SIAM Journal on Numerical Analysis*, 57, 1649–76.
- [36] Lesaint, P., & Raviart, P.-A. (1974). On a finite element method for solving the neutron transport equation. In *Mathematical Aspects of Finite Elements in Partial Differential Equations* (pp. 89–123. Publication No. 33). Math. Res. Center, Univ. of Wisconsin-Madison, Academic Press, New York.
- [37] Lučka, A. (1969). The rate of convergence to zero of the residual and the error for the Bubnov-Galerkin method and the method of least squares. In *Proc. Sem. Differential and Integral Equations, No. I (Russian)* (pp. 113–22). Kiev, Ukraine: Akad. Nauk Ukrain. SSR Inst. Mat.



- [38] Mozolevski, I., & Prudhomme, S. (2015). Goal-oriented error estimation based on equilibrated-flux reconstruction for finite element approximations of elliptic problems. *Computer Methods in Applied Mechanics and Engineering*, 288, 127–45.
- [39] Oden, J. T., & Prudhomme, S. (2001). Goal-oriented error estimation and adaptivity for the finite element method. *Computers & mathematics with applications*, 41, 735–56.
- [40] Prudhomme, S., & Oden, J. T. (1999). On goal-oriented error estimation for elliptic problems: application to the control of pointwise errors. *Computer Methods in Applied Mechanics and Engineering*, 176, 313–31.
- [41] Reed, W. H., & Hill, T. R. (1973). *Triangular mesh methods for the neutron transport equation*. Technical Report LA-UR-73-0479, <http://lib-www.lanl.gov/cgi-bin/getfile?00354107.pdf> Los Alamos Scientific Laboratory Los Alamos, NM.
- [42] Riviere, B. (2008). *Discontinuous Galerkin methods for solving elliptic and parabolic equations: theory and implementation*. SIAM.
- [43] Rivière, B., Wheeler, M. F., & Girault, V. (1999). Improved energy estimates for interior penalty, constrained and discontinuous galerkin methods for elliptic problems. part i. *Computational Geosciences*, 3, 337–60.
- [44] Romkes, A., Oden, J. T., & Vemaganti, K. (2006). Multi-scale goal-oriented adaptive modeling of random heterogeneous materials. *Mechanics of materials*, 38, 859–72.
- [45] Zitelli, J., Muga, I., Demkowicz, L., Gopalakrishnan, J., Pardo, D., & Calo, V. M. (2011). A class of discontinuous Petrov–Galerkin methods. Part IV: The optimal test norm and time-harmonic wave propagation in 1D. *Journal of Computational Physics*, 230, 2406–32.